Hippocampal Differential Gene Expression Converges Across Animal Models of Mood Disorder: Results from An Interactive Meta-Analysis Pipeline Encompassing Five Animal Models

A thesis submitted in partial fulfillment of
the Degree of Bachelor of Science in Neuroscience with Honors

December 1, 2022

Yusra Sannah

Mentors:

Megan Hagenauer, Ph.D., *Assistant Research Scientist, Michigan Neuroscience Institute*

Huzefa Khalil, Ph.D., *Postdoctoral Research Fellow, Michigan Neuroscience Institute*

Huda Akil, Ph.D., *Professor of Psychiatry and Gardner C. Quarton Distinguished University Professor of Neurosciences, Department of Psychiatry, Michigan Neuroscience Institute*

Reader and Co-Sponsor:

Dr. Jill Becker, Ph.D. *Patricia Y. Gurin Collegiate Professor of Psychology, Department of Psychology, Michigan Neuroscience Institute*

Reader:

Dr. Joanna Spencer-Segal, M.D., Ph.D. *Assistant Professor, Internal Medicine, Michigan Neuroscience Institute*

Abstract

The Hope for Depression Research Foundation (HDRF) brings together several research groups conducting transcriptomic studies in different animal models of depression. Since no single animal model is optimal at representing human depression, the convergence between them may point to key neurobiological mechanisms relevant to the regulation of mood. To facilitate this, an interactive meta-analysis pipeline was constructed to identify consistent gene expression signatures across custom-defined sets of animal models, conditions, transcriptional profiling platforms, and brain regions. To test this pipeline, we selected thirteen microarray and RNA-seq datasets derived from the hippocampus or dentate gyrus of five animal models: Selectively-bred High Responder and Low Responder rats, Flinders Sensitive and Resistant rats, glucocorticoid receptor overexpression mice, chronic social defeat stress mice, and chronic corticosterone-treated mice (total n=146). We found 27 candidate genes (FDR<0.1) which showed similar differential expression in the hippocampus across these animal models. These genes were highly skewed towards down-regulation (89%) and with particularly enriched expression in two hippocampal cell types: astrocytes (63%) and ependymal cells (30%). Gene Set Enrichment Analysis further indicated down-regulation within gene sets specific to the astrocytes, ependyma, choroid plexus, interneurons, polydendrocytes, and oligodendrocytes, and upregulation related to CA1 pyramidal neurons. These findings converge with results from post-mortem patients indicating reduced hippocampal astrocytic gene expression in depressed individuals, and thus illustrate the power of integrating results from numerous distinct animal models of depression to provide new avenues for investigating the neurobiology of this disorder.

Scientific Acknowledgements

This work was supported by funding to Drs. Huda Akil and Stanley J. Watson at the Michigan Neuroscience Institute (MNI), including the Hope for Depression Research Foundation, the National Institute on Drug Abuse (NIDA) U01DA043098, The Office of Naval Research (ONR) Grant N00014-12-1-0366, the National Institutes of Mental Health (NIMH) NCRR Grant R01MH104261, and the Pritzker Neuropsychiatric Disorders Research Consortium.

This project was carried out collaboratively with my two research mentors, Dr. Huzefa Khalil and Dr. Megan Hagenauer. I used the HDRF Gene Explorer, an online tool created by Dr. Huzefa Khalil, to run the meta-analysis and generate Figures 1, 2, and 3. The data included was also preprocessed by Dr. Khalil. I adapted code for running fGSEA from example code provided by Dr. Megan Hagenauer. The remaining figures and tables are my own creation, and the writing is my own, produced under the guidance of my mentors.

Finally, I should disclose that the formal methodological summaries that I wrote that are included in the Appendix have already been published on the HDRF website under "Model Information" and were partially used in fulfilment of a final paper requirement for PSYCH 420 - Faculty Directed Advanced Tutorial Reading for Psychology as a Natural Science.

Personal Acknowledgements

I would like to express my deepest gratitude to my mentor, Dr. Megan Hagenauer, for her immeasurable support, generosity, patience, and flexibility throughout my scientific research journey over the past three years. I cannot imagine a more suitable environment to explore my scientific interests and deepen my understanding of the field of neuroscience.

Thanks to both Dr. Megan Hagenauer and Dr. Huzefa Khalil for investing time in teaching me statistical coding. To Dr. Huzefa Khalil, thank you for introducing me to the essence of this project, the HDRF Gene Explorer, and for the opportunity to write the introductory information currently published on it.

I would like to thank my readers and co-sponsor Dr. Jill Becker and Dr. Joanna Spencer-Segal for taking the time to invest in my future through honest assessment of my work. Likewise, thanks to all of the Wakils for providing a welcoming environment and for sharing expertise about top genes from the meta-analysis output. Their insight helped set the foundation for my interpretation of the results.

I would also like to express a special thank you to Dr. Huda Akil for seeing my potential from so early on in my undergraduate career. Thank you for connecting me with my wonderful mentors and welcoming me in Wakil lab meetings. Our shared Syrian roots have inspired me to aim for excellence as you have accomplished so much as a pioneer of this field.

Table of Contents

Index of Figures

Index of Tables

Introduction

Depression is one of the most prevalent illnesses in the world, while also being one of the least understood. Approximately 350 million people worldwide suffer from depression, yet the current treatment is only 50% effective (Akil et al., 2018; James et al., 2018; Rush et al., 2006). This tremendous gap places a staggering weight on society. Not only is depression the leading cause of suicide, but it is also linked to a large economic burden via reduced work productivity and greater use of healthcare resources (Bachmann, 2018; Chow et al., 2019). The economic cost of adult patients diagnosed with Major Depressive Disorder (MDD) reached 286 billion USD in 2018 (Greenberg et al., 2021). Moreover, depression hinders family functioning, and can even imbue physical and psychological illnesses on family members of depressed patients (O′Donnell & Meaney, 2017, as cited in Akil et al., 2018; Keitner & Miller, 1990; Sobieraj et al., 1998). This tremendous toll felt at every level of society necessitates an improved understanding of the neurobiology of the disorder.

In 2010, the Hope for Depression Research Foundation (HDRF) formed to address the urgency for advancement towards improved treatments, and ultimately, a cure. HDRF established a multidisciplinary team of leading scientists from around the world, the Depression Task Force, to lead this effort. Their plan promotes a more collaborative, efficient, and expedited global initiative. The first step in this initiative, which remains ongoing, includes researching a variety of animal models to better understand the neural mechanisms underlying depression, using a collaborative approach between laboratories (*HDRF Gene Explorer*, 2022; *Research on Depression*, n.d.). Our current study includes five of the models used within HDRF: Chronic Social Defeat Stress mice (CSDS, vs. control), chronic corticosterone-treated rats (CORT, vs. vehicle-treated), selectively-bred Flinders Sensitive Line rats (FSL, vs. Flinders Resistant Line, FRL), glucocorticoid receptor overexpression mice (GRov, vs. control), and selectively-bred Low Responder rats (bLR, vs. bred High Responder rats, bHR).

HDRF supports a diverse array of models because no one animal model encompasses all aspects of depression. As the first part of this thesis, I will describe each of the models used by HDRF and the ways in which the models explore different aspects of depression. As the second

part of this thesis, I will discuss our efforts to find convergence in the neurobiology underlying the different animal models using a meta-analysis of hippocampal transcriptional profiling data.

The Animal Models of Depression Used Within HDRF

Scientists develop and validate animal models based on three main criteria: a) face validity; b) construct validity, and c) predictive validity (Belzung & Lemoine, 2011; Duman, 2010; Krishnan & Nestler, 2011a; Q. Wang et al., 2017). Face validity refers to the ability of an animal to mimic what is observed in the human disorder. Construct validity refers to the representation of the etiology, or mechanisms believed to cause the disease observed in humans. Finally, predictive validity (also known as pharmacological validity) describes the susceptibility of the model to known treatments that combat the human disease (Belzung & Lemoine, 2011; Duman, 2010; Krishnan & Nestler, 2011a; Q. Wang et al., 2017). Each depression model used by HDRF satisfies these criteria for validity in a different manner. We will discuss face validity and construct validity for each model in more detail below.

The Face Validity of the Animal Models of Depression Used Within HDRF

Face validity refers to whether an animal model exhibits what is observed in the human disorder (Belzung & Lemoine, 2011; Duman, 2010; Krishnan & Nestler, 2011a; Q. Wang et al., 2017). These observations are inclusive of anatomical, biochemical, neuropathological, behavioral and molecular phenotypes (Belzung & Lemoine, 2011; Duman, 2010; Krishnan & Nestler, 2011a; Q. Wang et al., 2017), but for modeling psychiatric disorder, great emphasis is placed on modeling cognitive and behavioral symptoms. In this sense, the face validity of animal models of depression can be a point of contention due to the diversity of depressive symptoms in human patients - there is no one marked feature or symptom that is present in all cases of depression. Moreover, a recent review points to a total of 681 possible combinations of symptoms that could meet the criteria for MDD (Akil et al., 2018), as defined by the Diagnostic and Statistical Manual of Mental Disorders (DSM-5) (*Diagnostic and Statistical Manual of Mental Disorders*, 2013). The criteria for MDD according to the DSM-5 include presenting a minimum of five of the symptoms shown in **Table 1**, some of which can manifest in opposing directions in different patients (e.g., hypersomnia vs. insomnia).

There is also no single animal behavior that models each symptom. Within **Table 1**, for each symptom of MDD we list the terminology used in animal model research to describe the effect, the common behavioral tests or methods of measurement from which the data is derived, and the expected results for animals with depressive-like symptoms (Krishnan & Nestler, 2011a; Q. Wang et al., 2017). Because there is no single behavior that defines depressive-like behavior, many experiments modeling depression in animals measure a variety of related behaviors ("behavioral battery"). These behavioral batteries typically include at least one test targeting either behavioral despair or behavioral anhedonia, which is defined as a persistent and severe lack of pleasure and motivation (Cooper et al., 2018). Since depressive disorders are highly comorbid with anxiety – nearly 75% of individuals with MDD also have anxiety-related disorders (Groen et al., 2020) – many behavioral batteries also measure anxiety-like behavior. Some of the tests most commonly used to demonstrate depressive-like behavior in the HDRF models are discussed in more detail below, along with the models exhibiting each behavior.

Modeling Depressive Symptoms in Animals: Behavioral Tests Commonly Used By HDRF

Behavioral Despair

The Forced Swim Test: The forced swim test (FST), first named the *Porsolt* test, assesses despair based on the rodent's drive to escape an inescapable container filled with water (Porsolt et al., 1977). Due to the nature of rodents, they typically strive to escape water to dry land. However, rats exhibiting depressive-like behaviors demonstrate much shorter attempts at escaping before accepting the situation, indicated by immobility, or the lack of movement beyond keeping the nose above the water level (Duman, 2010).

The FST has been widely used as a screening test for potential antidepressants. By observing the difference in immobility time, or the time it takes for an animal to relinquish escape efforts, between control groups and those with an antidepressant candidate, researchers can determine the efficacy of the antidepressant in the reversal of one aspect of depressive-like

behavior (Duman, 2010). Additionally, scientists are able to differentiate between antidepressant mechanisms of action based on the prevalence of distinct behaviors during the FST (Detke et al., 1995).

Current antidepressant medications increase the time of active escape response and thus decrease the time in a state of "despair". However, some scientists criticize the FST for wrongly anthropomorphizing animal behavior and accompanied by a lack of pathophysiological evidence (Nestler & Hyman, 2010). Moreover, a recent review article reveals that the success rate of the FST at identifying novel antidepressants is quite low (Trunnell & Carvalho, 2021). An important confound of the FST is the animal's innate tendency towards immobility, as seen in the bHR/bLR model (*discussed below*), which can conflate long times in behavioral despair with a disinclination toward movement (Estanislau et al., 2011, as cited in Bogdanova et al., 2013). Thus, reliance on FST as a stand-alone model of depressive symptoms itself has diminished over time, but it remains common practice to include it as a measure of depressive-like behaviors. Within HDRF, the animal models of depression that show depressive-like behavior by the FST include the CORT model, FSL model, GRov model, and bLR model (**Table 1**).

The Tail Suspension Test (TST): This paradigm characterizes behavioral despair through the suspension of mice by their tails in open space with behavioral analysis (Can et al., 2012). Similar to the FST, the results of the TST are quantified through immobility time vs. active escape behavior (Can et al., 2012). Within a 6-minute suspension duration, mice show distinctly longer immobility times when in a depressive-like state, which is reduced by antidepressant treatment (Can et al., 2012). However, the TST is limited by its specificity to mice and potentially confounded results based on motor deficits (Q. Wang et al., 2017). Rats are not tested with this paradigm due to their larger size and weight (Duman, 2010). This explains the lack of data from the TST for rat models of depression, including the FSL/FRL and bLR/bHR models. The animal models of depression used by HDRF that demonstrate behavioral despair through the TST include the CORT and GRov models, while CSDS models show no significant difference in immobility time compared to controls across multiple studies (Kinsey et al., 2007, as cited by Hammels et al., 2015; Krishnan et al., 2007).

Behavioral Anhedonia

Sucrose Preference Test: It is no secret that the consumption of sugar is a fundamental source of pleasure. Thereby, a reduced preference for sugar consumption in rodents is interpreted as evidence for diminished interest in pleasurable activities, i.e., anhedonia (Liu et al., 2018). Designed as a "two-bottle preference test", the sucrose preference test assesses the preference of a rodent for a sucrose solution compared to water by providing open access to both bottles and noting differences in solution intake (Liu et al., 2018). Within HDRF, the rodent models with altered stress physiology (CORT) or stress exposure (CSDS) demonstrate a reduced preference for the sucrose solution (*as seen in* ***Table 1*****).** The models of depression that are not directly stress-based, such as the models of genetic susceptibility to depression (FSL/FRL, bLR/bHR) only consistently demonstrate decreased sucrose preference following stress manipulations (**Table 1***)*.

Social Interaction Test: The social interaction test (SIT) places rats in an open arena with another rodent in a small mesh enclosure against one wall. The experimental rodent is monitored for the ratio of time spent interacting with the novel rat compared to the time spent avoiding it. Social interaction is measured as time spent in close proximity to the caged rat compared to the time spent in the corners of the enclosure, often referred to as "avoidance zones" (Birt et al., 2021). The bright, open enclosure is perceived as aversive by the animals and decreases social interaction (Fuchs & Flügge, 2006). The social interaction test measures propensity to interact vs. avoid an unfamiliar animal. This test relies on the underlying assumption that social interaction is a hedonic experience, therefore a lack of it is considered a measure of anhedonia. However, the results from the SIT are also confounded with the effect of anxiety, since the time spent in social interactions can be increased using anxiolytics (Yasumatsu, 1995). Within HDRF, the models that show depressive-like behavior by the SIT include CSDS, CORT, FSL, and bLR models (**Table 1**).

Anxiety-Like Behavior & Locomotor Activity

The Elevated Plus Maze: The Elevated Plus Maze (EPM) test consists of placing animals on an elevated, plus-sign shaped platform in which there is a center square and four protruding paths that are termed "arms" (Komada et al., 2008). The two opposite arms are enclosed by walls, and the other two arms are open with no railing or boundaries. The EPM tests for anxiety-like behaviors, based on the innate disinclination of rodents for elevation and exposed areas (Komada et al., 2008). Rodents are typically observed exploring the open arms when in this testing setup. A more anxious-like rodent, however, generally remains within the closed arms, scarcely even looking out beyond the center square (Pellow et al., 1985). Subjects are monitored using a computerized video tracking system to record behaviors such as latency to first enter the open arm, time spent in the three types of locations (open arm, enclosed arm, or center square), and the total distance traveled over the duration of the test (Stead et al., 2006). Within HDRF, the EPM highlights anxiety in the CSDS, CORT, GRov, and bLR animal models (**Table 1**).

The Open Field Test: The Open Field Test (OFT) is commonly used to measure both anxiety-like behavior and locomotor activity. In this test, animals are placed in the center of a large, flat, open top, walled, and brightly-lit enclosure. As the animal wanders *ad-libitum,* common behaviors include "wall hugging" (keeping to the sides of the enclosure) versus exploration away from the walls of the enclosure. The ratio of these two behaviors during the OFT provides insight on anxiety due to rodents' innate preference to avoid novel open spaces. Anxiety is quantified using the ratio of time spent "wall hugging" to that of activity out in the open. The result expected of a non-anxious rodent is exploration of the center area. A more anxious-like rodent would, in contrast, either remain frozen in a corner where it feels most safe, or it would keep one side against a wall while slowly edging around the enclosure (Krishnan & Nestler, 2011a). Within HDRF, only the bLR/bHR model demonstrates anxiety-like behavior as measured by the OFT (**Table 1**).

Both the OFT and the EPM identify anxiolytic drugs, providing predictive validity for their ability to measure anxiety-like behavior. Results from the OFT and related tests (SIT, EPM), however, can be confounded with locomotor activity, as animals that are simply less likely to move may sometimes generate similar results to that of anxious or anhedonic rodents. That said, changes in locomotor activity itself could be considered to model the symptom of psychomotor retardation or agitation in depression. Therefore, the OFT is also used to measure

locomotor behavior based on the total distance traveled. Within HDRF, models that demonstrate "depressive-like" behavior, based hypoactivity on the OFT, include FSL and bLR. Conflicting results have been shown in CSDS animals, and no significant difference in CORT or GRov animals has been demonstrated (**Table 1**).

Major Depressive Disorder Diagnostic Criteria	Animal Model Descriptors	Behavioral Measures	Expected Result for Mood Disorder	Chronic Social Defeat (CSDS, vs. CTRL)	Chronic CORT (vs. CTRL)	Flinders Sensitive Line (FSL, vs. FRL)	GROV (or iGROV, vs. WT)	bred Low Responder (bLR, vs. bHR)
Depressed mood most of the day, nearly every day, as indicated by either subjective report (e.g., feels sad, empty, hopeless) or observation made by others (e.g., appears tearful).	Learned Helplessness[1], behavioral despair [1], Hopelessness	Forced Swim Test (FST) Immobility	↑	↔	↑	↑	↑	↑
		Tail Suspension Test (TST) Immobility (*mice only*)	↑	↔	↑	NA	↑	NA
Markedly diminished interest or pleasure in all, or almost all, activities most of the day, nearly every day (as indicated by either subjective account or observation).	Anhedonia, aversion (dysphoria)	Sucrose Preference	↓	↓	↓	⇅, ↓*	ND	⇅ ↓*
		Sexual Behavior	↓	↓	↓	↔	ND	ND
		Social Interaction Test (SIT)	↓	↓	↓	↓	ND	↓
Significant weight loss when not dieting or weight gain (e.g., a change of more than 5% of body weight in a month), or decrease or increase in appetite nearly every day.	Changes in Weight or Appetite	Measured weight, weight gain, or appetite	↓	⇅	↓	↓	↔	↔
Insomnia or hypersomnia nearly every day.	Disrupted sleep or daily/circadian rhythms	Disrupted Sleep	✓	ND	ND	✓	ND	✓
		Disrupted circadian rhythm	✓	✓	✓	ND	✓	✓
Psychomotor agitation or retardation nearly every day (observable by others, not merely subjective feelings of restlessness or being slowed down).	Locomotor Activity	Open Field	↓	⇅	↔	↓	↔	↓
Fatigue or loss of energy nearly every day.	Grooming	Novelty Evoked Grooming, Splash Test, observed within SIT	↓	↔	↓	ND	ND	ND
Feelings of worthlessness or excessive or inappropriate guilt (which may be delusional) nearly every day (not merely self-reproach or guilt about being sick).	Impossible to model in animals	NA	NA	NA	NA	NA	NA	NA
Diminished ability to think or concentrate, or indecisiveness, nearly every day (either by subjective account or as observed by others).	Executive function: Attention, Decision, & Memory tasks	Spontaneous alternation T-maze, Morris water Maze Test	↓	↔	↓	ND	↔	↔
Recurrent thoughts of death (not just fear of dying), recurrent suicidal ideation without a specific plan, or a suicide attempt or a specific plan for committing suicide.	Roughly modeled in animals: Self-Injurious behavior	Observation	↑	ND	ND	ND	ND	ND
Measures of Anxiety	Thigmotaxis	Time Spent in Open Arms of Elevated Plus Maze (EPM)	↓	↓	↓	↔	↓	↓
		% time in center of Open Field Test (OFT)	↓	⇅	↔	ND	↔	↓
	Light Aversion	Time in Light Box	↓	ND	↓	↓	↓	↓
		Time in Dark Box	↑	⇅	↑	↑	↑	ND
	Defensive Behavior	Predator Odor, Social Defeat	↑	↑	↑	ND	ND	↑
References	[1] [2]	[2]		[2], [7], [10], [17] [18]	[2], [8], [11] [15] [16] [23] [26]	[2], [6], [9], [19], [22], [25]	[5] [12] [20]	[3], [4], [13] [14] [21]

Table 1. Comparison of Animal Models of Depression with Human Symptoms of Major Depressive Disorder.

As defined by the Diagnostic and Statistical Manual of Mental Disorders (DSM-5), a minimum of five of the above symptoms is required for the diagnosis of Major Depressive Disorder. Based on these symptoms, we listed the terminology used in animal model research to describe the effect, the common behavioral tests or methods of measurement from which the data is derived, and the expected results for animals with depressive-like symptoms. Given the high co-morbidity of MDD with anxiety (Groen et al., 2020), we have included anxiety measures as well. These aspects were compared across five animal models of depression used within HDRF: Chronic Social Defeat Stress (CSDS), chronic corticosterone (CORT), selectively-bred Flinders Sensitive Line rats (FSL), and selectively-bred Low Responder rats (bLR). The highlighted cells emphasize which models coincide with the expected directionality of the effect in mood disorders. The sideways arrow (↔) indicates that there was no significant difference found in the depressed model when compared to controls. The combined up and down symbol (⇅) indicates the presence of conflicting results across multiple studies. An asterisk (*) notes effects seen only after additional stress manipulations, not under basal conditions. Some of the symptoms of MDD are impossible to model in animals, as there is no means of data collection. This is denoted as "not applicable" (NA). Data not found in literature searches is listed as "no data" (ND). References for each of the models are listed in the final row. This chart directly compares models to one another and to human MDD to provide a broader view of the current state of animal depression model research. [1] (Krishnan & Nestler, 2011a), [2] (Q. Wang et al., 2017), [3] (Flagel et al., 2014), [4] (Stead et al., 2006), [5] (Q. Wei et al., 2004), [6] (Blaveri et al., 2010), [7] (Krishnan et al., 2007), [8] (Samuels et al., 2014), [9] (Overstreet & Wegener, 2013), [10] (Hammels et al., 2015), [11] (Sterner & Kalynchuk, 2010), [12] (Kolber et al., 2008), [13] (Stedenfeld et al., 2011), [14] (Birt et al., 2021), [15] (Badr et al., 2020), [16] (David et al., 2009), [17] (Meshalkina & Kalueff, 2016), [18] (Yu et al., 2011), [19] (Karabeg et al., 2013), [20] (Q. Wei et al., 2007), [21] (Widman et al., 2019), [22] (Ferreira-Nuño et al., 2002), [23] (Chan et al., 2017), [24] (Kerman et al., 2011), [25] (Melas et al., 2021), [26] (Ardayfio & Kim, 20060522).

Face Validity of Animal Models within HDRF

In summary, to better understand the face validity of animal models of depression used within HDRF, we compared the characteristic behaviors of each of the animal models with the symptoms of MDD in humans in **Table 1**. Depression manifests in highly variable, subjective, and oftentimes contradictory symptoms, encompassed both by the DSM-5 criteria (such as the diagnostic criteria for either insomnia or hypersomnia, or significant weight loss or weight gain). For this reason, I used a variety of symbols in **Table 1** to represent corresponding animal model characteristics. As can be seen, no one animal model encapsulates all symptoms of MDD in entirety. That said, all of the animal models used by HDRF show either learned helplessness or behavioral despair (excluding the CSDS model), as demonstrated through either the FST or Tail Suspension Test (TST), or the presence of a marker for anhedonia (excluding GRov), as often indicated by either the SIT or sucrose preference test. All models have some form of sleep or circadian rhythm dysregulation. All models also show elevated anxiety – either thigmotaxis (excluding FSL) or light aversion (excluding CSDS). None of these models, or any animal model, can represent human feelings such as worthlessness or guilt.

The Construct Validity of the Animal Models of Depression Used within HDRF

A model may have face validity, but reflect a similar response to an entirely different underlying molecular cause. In such a case, the model does not reveal the deeply rooted mechanism of the disease. Therefore, the second criteria is construct (*a.k.a.* etiologic) validity. This describes the representation of the etiology, or the mechanisms believed to cause the disease observed in humans (Kerman et al., 2011). This form of validity is the least developed area within animal models of depression research (Belzung & Lemoine, 2011; Duman, 2010; Krishnan & Nestler, 2011a; Q. Wang et al., 2017) because depressive disorders have diverse origins that stem from both genetic and environmental factors, and the relative influence of these origins varies (Hebda-Bauer et al., 2010). This heterogeneity creates many opportunities for distinct models of depression, including inducing depressive-like behavior using genetic modification, drug treatment, stress paradigms, or selective breeding (Bagot et al., 2017; Birt et al., 2021; Samuels et al., 2014; Q. Wei et al., 2012a).

Central to many of the models used in HDRF is stress and anxiety. The relationship between depression, anxiety, and stress is complex. Many studies report more than half of patients with depression also experience anxiety (Caffrey, 2017; Flint & Kendler, 2014; Melartin et al., 2002; Zimmerman et al., 2002, 2019). Some studies show that lifetime and 12-month MDD indicate 41-45% comorbidity with one or more concurrent anxiety disorders (Kalin, 2020; Kessler et al., 2015). There is also a high lifetime comorbidity of anxiety disorders with depression, ranging from 20-70% (Kalin, 2020). This comorbidity has lead researchers to group these disorders together under the general class of "internalizing disorders", which are characterized by anxious, depressive, and neurotic symptoms, as contrasted with "externalizing" psychiatric disorders, which are characterized by impulsivity and novelty-seeking behavior (Birt et al., 2021). Such comorbidity means that modeling depression requires parsing symptoms that are shared with anxiety disorders to better understand depression.

However, within MDD, anxiety onset specifically occurs before depression, suggesting that anxiety may not only be a co-morbidity, but part of the progression/development of depression in patients who are at high risk for internalizing disorders (Kessler & Wang, 2008). Comorbidity between depression and anxiety is associated with increased severity, as is seen across most psychiatric disorders comorbid with anxiety (Fava et al., 2004). This is demonstrated through increased suicidal ideation, increased debilitation through side effects of medication, and decreased likelihood of remission, among other factors (Fava et al., 2004, 2008). Further, anxiety is evidenced to impact depression treatments. In 2013, the DSM-V added an "anxiety distress specifier" to improve treatment plans based on the presence of anxiety, recognizing the significance and implications of anxiety on depression (Caffrey, 2017).

Likewise, both depression and anxiety, as well as other internalizing disorders, share genetic risk (Hettema, 2008). The estimated heritability of depression is reported to be approximately 40% (Flint & Kendler, 2014; Kalin, 2020). Based on family and twin studies, the high comorbidity of depression and anxiety is a result of genetic risk factors that are shared between these disorders (Flint & Kendler, 2014; Hettema, 2008). The high level of comorbidity between generalized anxiety disorder and MDD is ascribed to common genetics, as evidenced by generalized risk scores created with single nucleotide polymorphism data (Kalin, 2020). These genome-wide association studies demonstrate that genetic loci that increase susceptibility to depression do the same for anxiety.

However, heritability is not a standalone contributor. Depression and anxiety also share non-genetic risk factors, such as conditions involving trauma, neglect, and stress that is ongoing or early in life (Kalin, 2020). Chronic stress is one of the most common manners of inducing depressive-like behavior in animals *(discussed below).* Animals showing anxious-like behavior are more susceptible to stress paradigms that induce depressive-like responses (Krishnan & Nestler, 2011a; Q. Wang et al., 2017). Thus, many commonly-used genetic models of depression also have elevated anxiety and stress-susceptibility (*discussed below*), and may use stress within experiments to trigger or amplify depressive-like behavior.

Construction of Animal Models of Depression: Models within HDRF

Models of Genetic Susceptibility with HDRF

These models take into account the interplay of genetic and environmental factors in the development of depression. More specifically, depression is likely due, at least in part, to the inheritance of a disposition that makes some individuals more susceptible to the disease than others in similar environments. Therefore, genetic models of depression-susceptibility typically exhibit some depressive-like behaviors at baseline that are amplified under particular conditions, such as stress. That said, within the meta-analysis discussed later in this thesis, we did not include data from animal models of genetic susceptibility that were exposed to additional interventions beyond basal conditions and behavioral tasks.

The Selectively-Bred Low Responder (bLR) and High Responder (bHR) rat model

One behavioral trait that scientists have found predicts disposition/vulnerability to depressive-like behavior in rodents is locomotor activity in a novel environment (Flagel et al., 2014). Animals exhibiting low levels of exploratory activity are classified as Low Responders, and those on the opposite end of the spectrum are classified as High Responders (Flagel et al., 2014). By breeding rats that display these traits over generations, scientists develop bred lines of temperamental extremes as evidenced by consistent behavioral tracking (Birt et al., 2021; Flagel et al., 2014). The bred Low Responder (LR) vs. bred High Responder (bHR) model is generated via a selective breeding strategy. Sprague-Dawley rats are bred using the top and bottom 20% of

locomotor testing scores in order to emphasize the differences in phenotype between the two groups (Birt et al., 2021).

Although bLR/bHR rats are selectively bred based on locomotion in a novel environment, they show broader differences in overall temperament (Birt et al., 2021). The bHR group demonstrates a phenotype of aggressive, exploratory, and reward-seeking behavior (a model of externalizing disorders), while the bLR group exhibits anxious, less exploratory, depressive-like behavior and greater stress susceptibility (a model of internalizing disorders) (Birt et al., 2021; Flagel et al., 2014).

As shown in **Table 1**, the animal model descriptors of depressive-like symptoms that researchers find in bLR animals include learned helplessness (increased immobility in FST), anhedonia via decreased social interaction, disrupted sleep and circadian rhythm, and decreased locomotor activity. Measures of anxiety seen in bLR animals include decreased time spent in open arms of the EPM, decreased percent time in the center of the OFT, decreased time in the Light Box, and defensive behavior (**Table 1**).

Notably, this model is often viewed as a method of generating vulnerability to depression rather than modeling ongoing depression (Akil et al., 2018). For this reason, researchers often combine this model with a stress manipulation in order to induce certain depressive-like phenotypes that are not present basally (Akil et al., 2018). For example, bLRs generally do not demonstrate anhedonia in the sucrose preference test unless stress is administered. Interestingly, anhedonia is present in bLRs basally in other behavioral tests, such as in the SIT, where there is no cost to the animal, such as missing out on a food reward (**Table 1**). This reiterates the opportunity of using this model to study vulnerability to depressive-like behavior.

The Flinders Sensitive/Flinders Resistant Line (FSL/FRL)

This model of vulnerability to depression came about from manipulation of resistance to diisopropylfluorophosphate (DFP) in rats (Overstreet & Wegener, 2013), which was then discovered to produce behavior similar to the depressive-like phenotype seen in other animal models. The experimenters selectively bred rats to be resistant to DFP, which is an acetylcholinesterase agent, and despite their efforts to breed resistance, the animals became more sensitive to DFP (Overstreet & Wegener, 2013) and were labeled Flinders Sensitive Line. The other selectively bred strain resembled control Sprague-Dawley rats and was deemed Flinders

Resistant Line, or FRL (Overstreet & Wegener, 2013). The unexpected FSL phenotype demonstrated greater sensitivity to other cholinergic agonists primarily due to increased acetylcholine muscarinic receptor expression (Overstreet & Wegener, 2013). Behavioral observations led experimenters to notice striking similarities of FSL rats to humans with depression, including learned helplessness (increased immobility in FST), anhedonia (decreased social interaction), changes in weight or appetite, decreased locomotor activity (OFT), and disrupted sleep (specifically increased REM sleep) (Blaveri et al., 2010; Ferreira-Nuño et al., 2002; Overstreet & Wegener, 2013; Q. Wang et al., 2017) (**Table 1**). However, a noteworthy feature of the FSL model (similar to bLR) is the ability to trigger some depressive-like symptoms (i.e., anhedonia) after chronic mild stress (Pucilowski et al., 1993). Most characteristics, such as spontaneous anxiety or lack of exploration exist in these models basally (**Table 1)**, while behavioral tests presenting a cost (i.e., not receiving a reward) require stress to for animals to behave in the depressive-like manner. Finally, the FSL model also demonstrates light aversion in both Light and Dark Box tests, a measure of anxiety in animals (**Table 1**).

Models of Stress Exposure or Altered Stress Physiology within HDRF

Conditions involving trauma, neglect, and stress are risk factors for depression (Kalin, 2020), and can be easily modeled in the laboratory with animals. Stress circuitry can also be directly modified by experimenters to produce a heightened stress response.

Chronic Social Defeat Stress (CSDS)

Social defeat can be achieved through conflict between two animals at different levels in a social dominance hierarchy. An animal's place in this hierarchy can be induced by various factors, including by training, species, or size, but can also be established simply by natural tendency (Kollack-Walker et al., 1997). In the CSDS models used by HDRF, social defeat is induced through conflict between a smaller experimental rodent, and an older, larger, aggressor rodent trained to imbue feelings of anxiety, helplessness, and social ostracization by recurring defeat experiences (Krishnan et al., 2007). This encounter occurs in the aggressor's territory, creating an interaction where the smaller experimental rodent, or "intruder", is intimidated, cornered, and nearly attacked, with no escape or means of protection (Krishnan et al., 2007). The

intruder will assume submissive behavior, emit vocalizations of despair, and freeze (Krishnan et al., 2007). At the end of the defeat experience, the intruder is removed from this immediate source of stress (Krishnan et al., 2007). The psychological stress, however, continues as the victim is housed beside the aggressor, separated only by plexiglass (a transparent, perforated barrier), for the continuation of that day (Krishnan et al., 2007). This sustained sensory stimulation, inclusive of visual and olfactory stimuli, along with repeated social defeat experiences with novel aggressors, leads to the development of chronic stress (Krishnan et al., 2007). After experiencing CSDS, the animals diverge into two groups, "susceptible" or "resilient" (as measured by social interaction) despite coming from the same strain and similar genetic background (Golden et al., 2011). Whether the social interaction of some animals appears affected by CSDS is difficult to predict, but recent work has suggested that differences in initial coping mechanisms may play a role in this rift (Murra et al., 2022). One major weakness of the chronic social defeat stress model is that it is difficult to use with females due to the hallmark feature of territorial aggression between males (Krishnan & Nestler, 2011b).

Within HDRF, the chronic social defeat stress paradigm typically adheres to a procedure similar to the following. Aggressor CD-1 mice are pre-selected based on the benchmark of at least two attacks made on a C57BL/6J mouse within the first 60 seconds of the encounter. This screening process is often repeated to ensure the most aggressive mice are chosen as aggressors for the CSDS procedure. The CSDS paradigm is then typically conducted for 10 consecutive days, for 5–10 min/per day, after which the intruder is returned behind the perforated plexiglass divider for the remainder of the 24-hour period. Each social defeat occurs with a novel aggressor mouse.

Overall, the CSDS model demonstrates depressive-like characteristics in animals via hallmark effects of anhedonia and aversion (decreased sucrose preference, sexual behavior, and social interaction) and disrupted circadian rhythm, while also representing some aspects of anxiety-like behavior as well, such as thigmotaxis and defensiveness (**Table 1**). Notably, CSDS manipulation does not generate behavioral despair as seen by the lack of significant differences in the FST compared to controls, unlike the other animal models of depression discussed (**Table 1**). A review by Wang et al. reinforces this notion by describing CSDS models as only emulating anxious and anhedonic symptoms, not despair/hopelessness (Q. Wang et al., 2017).

Chronic Corticosterone (CORT)

Patients with MDD experience a hyperactive limbic-hypothalamic–pituitary–adrenal (LHPA) axis, resulting in excess cortisol released into the blood (McEwen & Akil, 2020). The LHPA axis is a neuro-endocrine mechanism that mediates the biological response to stressful experiences (McEwen & Akil, 2020). The perception of a threat leads to a converging signal activating the paraventricular nucleus of the hypothalamus to release corticotropin releasing hormone (CRH) into hypothalamo-pituitary portal vessels to act on the anterior pituitary gland (McEwen & Akil, 2020). CRH stimulates the anterior pituitary to release adrenocorticotropic hormone (ACTH) into the venous circulation, which promotes glucocorticoid (including cortisol, or corticosterone in rodents) secretion from the adrenal cortex (McEwen & Akil, 2020). Glucocorticoids then travel throughout the body to stimulate the many reactions associated with the stress response, but also inhibit production of both CRH and ACTH in a negative feedback loop (McEwen & Akil, 2020). Feedback inhibition of the HPA axis also involves the hippocampus, which densely expresses receptors for stress hormones, known as glucocorticoid receptors (GR) (McEwen & Akil, 2020, Q. Wei et al., 2004). The extent of receptor expression modulates inhibition, contributing to dysregulation of the stress response (Q. Wei et al., 2004) (*discussed below*).

To mimic HPA axis imbalance in animal models, researchers elevate CORT levels either through injections or chronic oral treatment via drinking water *ad libitum*. The study used in the meta-analysis discussed later in this thesis implemented a six-week chronic oral treatment (*Appendix 1*). This chronic treatment generates both anxiety-like and depressive-like behavior (Badr et al., 2020; Berger et al., 2019; Caradonna et al., 2022; Dieterich et al., 2019). The observations that support this include characteristics of learned helplessness (in both FST and TST), anhedonia (as in low sucrose preference, low sexual behavior, and low social interaction), changes in weight/appetite, disrupted circadian rhythm, lack of grooming, and executive function deficits (**Table 1**). This model also exhibits anxiety-like behaviors in animals including thigmotaxis (decreased time spent in open arms of EPM), light aversion (Light and Dark Box), and defensive behavior (**Table 1**).

However, much of the data linking dysregulation of the HPA axis to depression is only correlational. Despite mounting clinical evidence supporting the link, researchers are unable to distinguish whether a high plasma cortisol concentration is a cause or effect of depression

(Sterner & Kalynchuk, 2010). This highlights the importance of studying the chronic CORT model and others with altered stress physiology.

Glucocorticoid Overexpression (GRov)

The Glucocorticoid Overexpression (GRov) animal model is an example of a genetic approach to modeling the relationship between stress biology and emotional reactivity. This model, similar to the CORT model, stems from the understanding that the hypothalamic–pituitary–adrenal (HPA) axis is implicated in stress responsiveness and is dysregulated in humans with depression (Q. Wei et al., 2004). The final step of the LHPA axis, as described above, is the synthesis and secretion of stress hormone known as glucocorticoids from the adrenal cortex (McEwen & Akil, 2020). In turn, these hormones mediate the negative feedback on the LHPA axis via glucocorticoid receptors (GRs) throughout the brain (McEwen & Akil, 2020). In the forebrain, GRs act as a "stress sensor" that regulates the neural circuits relating to stress responsiveness, including anxiety-like responses that impact learning and memory (Kolber et al., 2008). Studies show that forebrain-specific GR overexpression causes animals to exhibit increased emotional range and lability, anxiety, and depressive-like behavior (Q. Wei et al., 2004). This can be measured by an animal's change in behavior to represent more caution and less risk-taking behavior, indicated by behavioral testing such as the FST and EPM (**Table 1**). Another study by Wei et. al investigating whether the timing of GR overexpression plays a role in the phenotype found that overexpression of GR early in the lives of the animal subjects was not only necessary to lead to the Grov phenotype, but also the only period that was sufficient to induce the phenotype alone, unlike any other life period (Q. Wei et al., 2012).

The characteristic behaviors that make the GRov mouse model "depressive-like" include learned helplessness/behavioral despair (increased immobility in FST and TST) and disrupted circadian rhythm (**Table 1**). The behaviors of GRov that play into measures of anxiety include thigmotaxis and light aversion (**Table 1**).

Conclusion: How Well is Depression Modeled in HDRF?

As can be seen, no one animal model within HDRF is optimal at representing human depression. No model encapsulates all symptoms of MDD in entirety, but all of the animal

models used within HDRF show a variety of behaviors that are used to model depressive symptoms in humans. All of the animal models used by HDRF show either learned helplessness or behavioral despair or anhedonia. All HDRF models also have elevated anxiety and some form of sleep or circadian rhythm dysregulation. However, none of the HDRF models can represent the uniquely human feelings of worthlessness or guilt. The models within HDRF are also constructed to target different pathways to depression, although they are skewed towards representing depressive-like behavior induced by genetic susceptibility, stress, or alterations in stress physiology. This skew is representative of the field as a whole - most animal models used in depression research focus on stress reactivity and its potential to trigger or shape affective changes. These aspects of depression are important, but future efforts by HDRF should include models representing other pathways to depression including inflammation and insulin resistance.

Finally, as no single animal model is optimal at representing human depression, the convergence between them may point to key neurobiological mechanisms in emotional reactivity that are likely to be relevant to the regulation of mood in humans.

Using a Meta-Analysis of Transcriptional Profiling Studies from HDRF Models to Explore the Neurobiology of Depression

Our project aimed to incorporate data across multiple animal models of depression, focusing on models based on altered stress reactivity and genetic vulnerability, to reveal underlying convergence. By doing so, we hoped to expose the neurobiological mechanisms most likely to be relevant to the regulation of mood disorder. To facilitate comparison of the neurobiological signatures across different models of depression, we drew from the HDRF Data Center, a centralized databank collecting results from associated labs since 2014, focusing on transcriptional profiling data.

Based on the availability of data from different brain regions in the HDRF Data Center, we selected the hippocampus (HC) as our focus. The hippocampus is a useful brain region for providing insight into depression due to its involvement in emotion, psychosocial stress, and mood disorders (Dranovsky & Hen, 2006). Patients with depression often have a smaller hippocampus, with evidence showing progressive atrophy in depressed patients (Dranovsky & Hen, 2006)(Sheline et al., 1996). A meta-analysis of MRI studies of unipolar depression found a

significant reduction of hippocampal volume of up to 10%, concluding that this might the be a result of multiple exposures to MDD (Videbech & Ravnkilde, 2004). Volume reductions also correlate with MDD progression markers, indicating that they are a consequence of depression, but there remains a debate regarding whether reductions might also be a cause for depression onset (Belleau et al., 2019; Treadway et al., 2015). Longitudinal studies show that common antidepressants counteract the loss of hippocampal volume found in depression, and yet depressed brains still show a significant volume reduction (Belleau et al., 2019).

The hippocampus is also highly sensitive to stress. The hippocampus mediates negative feedback regulation of glucocorticoid release via dense expression of glucocorticoid receptors on hippocampal neurons that signal inhibition of glucocorticoid release (McEwen et al., 1968). Patients with MDD exhibit high blood levels of glucocorticoids due to a loss of inhibition from the diminishing hippocampal volume (Anacker et al., 2011).

For these reasons, the hippocampus is central to the study of depression and a worthy focus of this meta-analysis. The hippocampus is divided into subregions, including the dentate gyrus, which is one of two areas of the brain where neurogenesis occurs throughout adulthood, making it especially plastic. Due to this characteristic, we included data specifically derived from the dentate gyrus as a part of this analysis, as well as data derived from the dorsal or ventral hippocampus as a whole.

An Introduction to Transcriptional Profiling

In order to understand the data collected in this study, it is necessary to briefly introduce the basic principles of transcriptional profiling technology. Transcriptional profiling technology is based on the central dogma of molecular biology: the idea that DNA is the blueprint for RNA, which encodes proteins, which carry out life processes (X. Wang, 2016). Transcription describes the first transmission of genetic information from DNA to RNA (X. Wang, 2016). Since all cells of the same organism contain the same script of DNA, biological differences first arise from transcription (X. Wang, 2016). Regulation of transcription is one of many biological mechanisms that allow cells to differ in structure and function (X. Wang, 2016). Genes, or units of genetic information, can be transcribed at varying levels. Transcriptional profiling identifies which genes are active and how actively they are being transcribed (X. Wang, 2016). The level of

transcription of a gene can reveal information about the cell type and what chemical processes a given cell is prioritizing at a particular moment in time (X. Wang, 2016).

Transcription gives rise to multiple forms of RNA, which carry information for the synthesis of proteins out into the cytoplasm. This includes mRNA, rRNA, tRNA, to name a few. The principal form of RNA that holds the sequence for protein coding is mRNA, while rRNA and tRNA are vital for translation, working together to synthesize proteins based on the mRNA sequence (X. Wang, 2016).

Rather than being a rigid process, DNA transcription is influenced by environmental factors, causing biological differentiation even between organisms with identical DNA (X. Wang, 2016). Changes in transcription affect cellular levels of RNA transcript, and quantifying the amount of transcript ("gene expression") for the thousands of genes expressed in a sample is called transcriptional profiling (X. Wang, 2016). By comparing the transcriptional profiles of two distinct biological samples, we can observe how both nature and nurture interact to shape the biology of an organism. The method used to determine whether the gene expression from two conditions differ beyond what would be expected by random chance is called a differential expression (DE) analysis.

With the sheer amount of information gathered through transcriptional profiling, differential expression analyses typically take an unbiased, discovery-based approach rather than a hypothesis-driven one, and set broad aims to lay the foundation for future study. This approach seems particularly useful in the context of animal models of depression, as the lack of information known about the biological underpinnings of depression makes it unlikely that we can fully hypothesize the secrets of the depressed brain. Using a discovery approach in the context of animal models can point to new mechanisms that underlie either the vulnerability to depression or the impact of the illness on the brain. Our current study centered on transcriptional profiling studies from models generated by HDRF.

The HDRF Gene Explorer Meta-Analysis Tool

To identify convergence in the transcriptional profiling data across multiple animal models of depression, we used the new HDRF Gene Explorer (*HDRF Gene Explorer*, 2022), which allows researchers to efficiently run statistical analyses across studies of differential gene

expression in animal models of depression conducted by HDRF-associated labs within the HDRF Data Center. The website holds four main tools: a Results Viewer, a Data Download tool, a Meta-Analysis tool, and a tool to conduct Rank Rank Hypogeometric Overlap (RRHO). In addition to addressing our scientific goals, this project served as a beta-test for the HDRF Gene Explorer meta-analysis tool, both demonstrating utility and compiling the necessary supportive documentation for release.

Meta-analysis is a tool of particular importance in neuroscience research due the common usage of small sample sizes (typically 3-12 animals per group, Hagenauer M.H., 2022, *personal communication*). These small sample sizes hamper the ability to glean strong trends from individual studies by increasing the probability of both false negatives and false positives (Button et al., 2013). Such sample sizes are particularly common in transcriptional profiling studies (*i.e.*, RNA-Seq, microarray) due to processing costs. Therefore, combining multiple, similar datasets within a meta-analysis provides a more robust sample size for statistical analyses and paves the way for future research.

Previous Meta-analyses of Transcriptional Profiling Data from Depression Models

Our project is not the first to tackle this topic. Two recent meta-analyses have also combined microarray and RNA-Seq data to identify consistent hippocampal differential gene expression signatures related to chronic stress, a commonly used model of depression (Gui et al., 2021; Stankiewicz et al., 2022). One of these meta-analyses included 79 animal model studies of stress and 3 human studies of post-traumatic stress disorder, totaling 223 stress-control comparisons across three species, and identified significant overlap between animal models and human data (Stankiewicz et al., 2022). Another recent meta-analysis of hippocampal transcriptional profiling studies combined both animal models and human MDD patients, but focused solely on three stress-based animal models (chronic social defeat stress, chronic unpredictable mild stress, learned helplessness) (Gui et al., 2021). Both Gui et al. and Stankiewicz et al. used a popular meta-analysis method of quantifying overlap amongst the top differentially expressed genes identified in individual studies, which predominantly captures genes with the most prominent differences. Understanding the full picture of transcriptional differences in depression models requires a more inclusive powerful analytic technique: a meta-analysis of effect sizes of all genes from the various studies.

Another meta-analysis of transcriptional profiling data from animal models of depression focused exclusively on cortical areas of the brain (Reshetnikov et al., 2022). This meta-analysis used RNA-seq data from the pre-frontal cortex (PFC) of CSDS models in addition to post-mortem samples from patients with PTSD or MDD (Reshetnikov et al., 2022). Although this meta-analysis focused exclusively on cortex, some of their analysis methods were more similar to our current study than the hippocampal meta-analyses mentioned above, including an analysis estimating differential expression effect size for each gene across included studies.

Unlike these recent meta-analyses of stress-related models, we examined models of depression more broadly. We ran a formal meta-analysis of transcriptional profiling data comparing hippocampal brain tissue from five diverse animal models of depression to better understand the biological differences between normal and depressed brains. Each of the five models we included uses one of the following methods of inducing depressive-like behavior in rodents, including social defeat stress, glucocorticoid hormone exposure, selective breeding, and genetic modification. These models include animals from two different species and across multiple laboratories, and focused on tissue from areas within the hippocampus. Our goal was to both increase the effective statistical power of the transcriptional profiling studies and identify convergent differential gene expression among them.

Materials and Methods

Overview of Methods

To complete these goals, I conducted a meta-analysis across hippocampal transcriptional profiling studies of animal models of depression using the HDRF Gene Explorer Tool created by Dr. Huzefa Khalil in 2020 (R package *shiny*, v.1.7.1) and hosted on the HDRF Data Center website, built by Manhong Dai, Andy Lin, Fan Meng. The HDRF Data Center provided a starting point: the tool uses preprocessed data from experiments overviewed in **Table 2** *(further detailed in the Appendix 1).*

Model	Study	Dataset Name	Data Type	Species & Strain	Brain Region(s) Analyzed	Selective Breeding	Genetic Modification	Stress	Drug Treatment	Housing	Behavioral Measurements	Sample Sizes	Platform	Dissection Method
GRov	Wei et al. 2007	Akil-1	Microarray	Mus musculus C57BL/6J mice	Hippocampus (HPC) Striatum (STR) Prefrontal Cortex (PFC) Nucleus Accumbens (NAC)	--	Transgenic overexpression of GR in forebrain	--	--	--	--	**GRov n=5, WT n=6**	Affymetrix Mouse Genome 430_2.0 GeneChips	Dissected whole
GRov	Wei et al. 2012	Akil-4	Microarray	Mus musculus C57BL/6J mice	Dentate Gyrus (DG) and Nucleus Accumbens (NAC) and Cornu Ammonis (CA)	--	Inducible transgenic overexpression of GR in forebrain	--	± Doxycycline (Dox) (200 mg/kg chow)	--	--	**DG LT n=6, DG EL n=6, DG Control n=6** NAC LT n=7, NAC EL n=6, NAC Control n=6, CA Control n=4, CA EL n=6, CA LT n=7	Affymetrix Mouse Genome 430_2.0 GeneChips	Laser capture microdissection (LCM)
FSL/FRL	Blaveri et al. 2010	GSE20388	Microarray	Rattus Norvegicus Sprague-Dawley	Hippocampus (HPC) and Prefrontal/Frontal Cortex (P/FC)	Bred by resistance & hypersensitivity to DFP	--	--	--	--	Forced Swim Test (FST)	FRL FC n=22, **FRL HPC n=22**, FSL FC n=17, **FSL HPC n=17**	Affymetrix Rat Genome 230 2.0 GeneChips	Dissected whole
FSL/FRL	Bigio et al. 2016	McEwen-4	RNA-seq	Rattus norvegicus	Ventral Dentate Gyrus (vDG)	--	--	Acute stress during LAC treatment	LAC (sigma, 0.3% wt/vol) or tap water (vehicle)	--	Open Field Test, Forced Swim Test	**rFSL n=3, nrFSL n=3, vehicle FSL n=3, and vehicle FRL n=3**	Illumina HiSeq 2500 (100bp)	Micro-dissection
CORT-FLX	Samuels et al. 2014	Hen-1	Microarray	Mus musculus C57BL/6Ntac	Dorsal Dentate Gyrus (dDG) and Ventral Dentate Gyrus (vDG)	--	--	--	Corticosterone (35 ug/ml) dissolved in vehicle (0.45% beta-cyclodextrin) and FLX (160 ug/ml)	--	Novelty Suppressed Feeding Test (NSF) and Forced Swim Test (FST)	dDG Resistant n=4, dDG Responder n=7, vDG Resistant n=4, vDG Responder n=7, dDG non-FLX-treated control group n=8, vDG non-FLX-treated control group n=8	Affymetrix 430_2 3' expression arrays	Micro-dissection
CSDS	Bagot et al. 2016	Nestler-3	RNA-seq	Mus musculus C57BL/6J	Nucleus Accumbens (NAC), Ventral Hippocampus (vHIP), Prefrontal Cortex (PFC), and Amygdala (AMY)	--	--	Chronic social defeat stress	--	--	A two-stage social-interaction test for separation into resilient & susceptible groups	NAC: 48hr pCSDS n=3, Control 48hr n=3, 28d pCSDS n=4, Control 28d n=4, 28d1hr stress n=4, Control 28d + 1hr n=4. **vHIP: 48hr pCSDS n=3, Control 48hr n=3, 28 day pCSDS n=4, Control 28d n=4 28d+1hr stress n=4, Control 28d1hr n=4.** PFC: 48hr pCSDS n=3, Control 48hr n=3, 28d pCSDS n=4, Control 28d n=4, 28d + 1hr stress n=4, Control 28d1hr n=4. AMY: 48hr pCSDS n=3, Control 48hr n=3, 28d pCSDS n=4, Control 28d n=4, 28d + 1hr stress n=4, Control 28d1hr n=4	Illumina HiSeq 2500 System (100 bp)	15 g punch dissections for each region
CSDS	Bagot et al. 2017	Nestler-1	RNA-seq	Mus musculus C57BL/6J	Nucleus Accumbens (NAC), Ventral Hippocampus (VHPC), Prefrontal Cortex (PFC), and Amygdala (AMY)	--	--	Chronic social defeat stress	Imipramine (20 mg/kg), ketamine (10 mg/kg), or saline	--	A two-stage social-interaction test for separation into resilient & susceptible groups	PFC_CS n=5, PFC_RS n=4, PFC_SS n=3, PFC_SKR n=3, PFC_SKNR n=3 PFC_SINR n=3, PFC_SINR n=4, NAC_CS n=5, NAC_RS n=4, NAC_SS n=3, NAC_SKR n=3, NAC_SKNR n=3, NAC_SIR n=3, NAC_SINR n=4, **HIP_CS n=4**, HIP_RS, **HIP_SS n=3**, HIP_SKR n=3, HIP_SKNR n=3, HIP_SIR n=3, HIP_SINR n=4, AMY_CS n=5, AMY_RS n=4, AMY_SS n=3, AMY_SKR n=3, AMY_SKNR n=3, AMY_SIR n=3, AMY_SINR n=4	Illumina HiSeq 2500 System (50 bp)	15 g punch dissections for each region
CSDS	Caradonna et al. 2022	Meaney-2	RNA-seq	Mus musculus C57BL/6J	Ventral Dentate Gyrus (vDG)	--	--	Chronic social defeat stress	--	Enriched and standard	Light-Dark Box Test, Splash Test, Social Interaction Test	Enriched-Control n=10, **Standard-Control n=10**, Enriched-Resilient n=9, Standard-Resilient=7, Enriched-Susceptible=9, **Standard-Susceptible=10**	Illumina HiSeq 2500 (100bp)	300 µm diameter punch dissections
bHR/bLR	Birt, Hagenauer, et al. 2020	Akil-5	RNA-seq	Rattus Norvegicus Sprague-Dawley	Hippocampus (HIP)	37th gen (by locomotor activity to a novel environment)	--	--	--	--	Elevated Plus Maze (EPM)	**bHR n=6, bLR n=6**, bIR n=6	Illumina HiSeq 2000 (100bp)	Dissected whole
bHR/bLR	Birt, Hagenauer, et al. 2020	Akil-6	RNA-seq	Rattus Norvegicus Sprague-Dawley	Hippocampus (HIP)	43rd gen (by locomotor activity to a novel environment)	--	--	--	--	Elevated Plus Maze (EPM), Social Interaction testing	**bHR n=5, bLR n=5**	Illumina HiSeq 2000 (50 bp)	Dissected whole
BDNF Val66Met + CORT	Caradonna et al. 2022	McEwen-5	RNA-seq	Mus musculus C57BL/6J	Ventral Hippocampus (vHIP)	--	SNP of human BDNF gene Val66Met	--	25 µg/ml CORT dissolved in ethanol, diluted in tap water to 1% concentration	--	Light-Dark Box Test, Splash Test, Social Interaction Test	BDNF CORT n=3, **WT CORT n=3**, BDNF Saline n=3, **WT Saline n=3**	Illumina NextSeq 500 (75bp)	Immediate separation of VHIP upon dissection
BDNF Val66Met	Marrocco et al. 2020	--	RNA-seq	Mus musculus C57/BL6	Ventral Hippocampus (vHIP)	--	SNP of human BDNF gene Val66Met	--	Estradiol (0.7 g/day) or 0.1% ethanol (vehicle) for ovariectomy; ketamine (75 mg kg-1) xylazine (7.5 mg kg-1)	--	Open Field Test, Splash Test	BDNF E2 n=3 per group, BDNF Control n=3 per group	Illumina NextSeq 500 (75bp)	Dissected whole

Table 2. Characteristics of Datasets Available within the HDRF Data Center.

Each study in the HDRF meta-analysis website is represented as a dataset, grouped by model, and named using the name of the lab and a number (e.g., Akil-1). The species, strain, brain region, model description, housing, behavioral measurements, sample size, platform, and dissection method are described. The bolded sample sizes reflect the samples used in our comparisons described below, with respect to all of the available samples in the HDRF Gene-Explorer. Abbreviations: GRov (Glucocorticoid Receptor Overexpression,) FSL/FRL (Flinders Sensitive Line/Flinders Resistant Line), DFP (anticholinesterase diisopropylfluorophosphate), LAC (acetyl-l-carnitine), CORT (Corticosterone), CSDS (Chronic Social Defeat Stress), bHR/bLR (bred High Responders/bred Low Responders), HPC (Hippocampus), NAC (Nucleus Accumbens), FC (Frontal Cortex), EL (Early Life), LT (Lifetime), rFSL(responder FSL), nrFSL (nonresponder FSL), FLX (fluoxetine), WT (Wild Type), E2 (estradiol), SNP (Single-nucleotide polymorphism), CS (Control Saline), SS (Susceptible Saline), SKR (susceptible ketamine responder), SKNR (susceptible ketamine nonresponder), SIR (susceptible imipramine responder), SINR (susceptible imipramine nonresponder).

Inclusion & Exclusion Criteria

We included data from all depression models within the HDRF database, including GRov, bHR/bLR, FSL, CORT, CSDS. From the corresponding studies, we selected those that included a control or wild type (WT) group for comparison. Data from the hippocampus, ventral hippocampus, dentate gyrus, and ventral dentate gyrus were included. We included both mouse and rat data. Female data was excluded due to previous evidence of sex differences in the HDRF transcriptional profiling data (Labonté et al., 2017) and minimal representation in the database (n=4). We chose to only include animals that had not received drug treatment due to concerns that antidepressant interventions might obscure the differential expression associated with our depression models. This included both untreated and vehicle treated animals. For the experiment from Bagot et al. 2016 (Bagot et al., 2016), only the timepoints 28-day post CSDS, 28-day post CSDS + 1 hour stress, and 48-hour post CSDS were selected based on the social interaction scores for these groups indicating depressive-like behavior (Bagot et al., 2016).

For all studies, the included group comparisons were structured with the "depression-like group" minus the control or wild type group. This general convention makes it easy to interpret the results in terms of what genes were upregulated and downregulated in the "depression-like" group, with the downregulated genes on the left half of the volcano and forest plots, while upregulated groups would be on the right. **Table 3** shows a list of the specific comparisons included in our meta-analysis.

Despite the broad characteristics of our data inclusion, we excluded some datasets and comparisons from our meta-analysis. We excluded the dataset Hen-1 because it lacked a control group without depressive manipulation, as the comparisons in this study were tailored to discern the effect of antidepressant treatment rather than the effect of the CORT model. We also excluded the "Standard.Susceptible – Standard.Control" (vHPC) comparison from the Nestler-1 datasets (Bagot et al., 2017) due to its inclusion in the more general "Susceptible – Control" comparison already present in our meta-analysis. The "standard" group represents the subgroup kept in standard housing, compared to others that were not.

The final sample size reached a total of 146 animals (**Table 2**).

Study	Dataset Name	Comparisons
Wei et al. 2007	Akil-1	GRov - WT (HPC)
Wei et al 2012	Akil-4	EL.GRov - Control (DG) LT.GRov - Control (DG)
Birt, Hagenauer, et al. 2020	Akil-5	bLR - bHR (HPC)
Birt, Hagenauer, et al. 2020	Akil-6	bLR - bHR (HPC)
Blaveri et al. 2010	GSE20388	FSL - FRL (HPC)
Bigio et al. 2016	McEwen-4	FSL- FRL (vDG)
Caradonna et al. 2022	McEwen-5	CORT.WT- Saline WT (vHPC)
Caradonna et al. 2022	Meaney-2	Susceptible - Control (vDG)
Bagot et al. 2017	Nestler-1	Susceptible.Saline - Control.Saline (vHPC)
Bagot et al. 2016	Nestler-3	Susceptible - Control (vHPC, 28 days post CSDS) Susceptible - Control (vHPC, 28 days +1 hour stress post CSDS) Susceptible - Control (vHPC, 48 hours post CSDS)

Table 3. Comparisons Included in Meta-Analysis

Out of a total of ten datasets, from five laboratories, these thirteen group comparisons diverge in multiple ways. These comparisons encompass five animal models of depression, including three GRov comparisons, two bHR/bLR comparisons, two FSL/FRL comparisons, one CORT comparison, and five CSDS comparisons. The transcriptional profiling data reflected in these comparisons was collected in two ways: nine RNA-Seq and four microarray comparisons. The comparisons are from two different species, of which four came from Rattus norvegicus (Sprague-Dawley) and the remaining nine comparisons came from Mus musculus (C57BL/6J). The dissection methods also varied among these comparisons, with 4 comparisons specifically focused on the dentate gyrus (DG) subregion of the hippocampus. The final sample size reached a total of 146 animals.

Transcriptional Profiling

Overview

The transcriptional profiling studies were performed using either RNA Sequencing (RNA-Seq) or microarray. Prior to the transcriptional profiling itself, all of the hippocampal tissue from each study was extracted rapidly. Each study followed a specific protocol of either whole hippocampal dissection, laser capture microdissection, or punch dissection (**Table 2**). The RNA was extracted from the samples using extraction and isolation kits (detailed in *Appendix 1*). For RNA-Seq, the RNA was purified to deplete rRNA and tRNA prior to sequencing, as mRNA is only approximately 5% of the total RNA sample (Kukurba & Montgomery, 2015). Then, following purification, the RNA was broken into smaller fragments in order to be processed by the sequencer. In both RNA-Seq and microarray procedures, the next step of transcriptional profiling was library construction (X. Wang, 2016), during which the RNA fragments were reverse transcribed into complementary DNA (cDNA) for increased stability (X. Wang, 2016).

Microarray

In some of our included studies, microarray was used to quantify relative gene expression by measuring hybridization to a microarray chip. To do this, during the cDNA library

construction step, researchers attached one fluorescent label to each fragment of cDNA for identification by sample (Trachtenberg et al., 2012). Fluorescently labeled cDNA bound to probes anchored on the microarray chip, making use of the inherent quality of DNA known as hybridization: single stranded DNA annealed to complementary sequence via hydrogen bonding patterns (Trachtenberg et al., 2012). These microarray chips included probes representing the complementary sequences for thousands of potential cDNAs (Trachtenberg et al., 2012). The microarray chips were then washed to remove any extraneous, unhybridized cDNA and placed into a machine for data acquisition (Trachtenberg et al., 2012). The machines scanned the chips with a laser and measured the fluorescent light intensity in the images to discern the presence and amount of cDNA bound to each probe location (Trachtenberg et al., 2012). The quantity of bound cDNA reflecting the mRNA sequence that represented a specific gene indicated relatively how much that gene was expressed or not expressed (Trachtenberg et al., 2012).

There are different platforms used to collect microarray data. Our studies used the Affymetrix Mouse Genome 430_2.0 GeneChips or the Affymetrix Rat Genome 230 2.0 GeneChips (Affymetrix, Santa Clara, CA) *(see Appendix 1 for more details).*

Microarray Data Preprocessing

Prior to running our meta-analysis, all data was preprocessed using a similar pipeline. The microarray data was extracted from the HDRF data center or from the Gene Expression Omnibus repository using the R package *GEOQuery* (v.2.64.2). The data from the .CEL files representing the fluorescence at each probe location on the microarray chip was read into an AffyBatch using *ReadAffy()* (R package *Affy* v.1.74.0). Individual probes were annotated using a custom chip definition file (.cdf, http://brainarray.mbni.med.umich.edu/Brainarray/Database/CustomCDF/CDF_download.asp, v24, (Dai et al., 2005)) and then the data was summarized into probesets, background-corrected, log-transformed, and quantile normalized using Robust Multi-Array Average (function *rma()* in R package *Affy* v.3.15, default parameters). No batch corrections were applied. The R package *arrayQualityMetrics* (v.3.52.0, default parameters) was used to define low-quality samples, leading to the exclusion of samples within the Akil-1 dataset (**Table 2**) including three GRov samples from the hippocampus, nucleus accumbens, and striatum. We also excluded two control

samples from the CA brain region and one sample from the nucleus accumbens EL GRov group within Akil-4 dataset. No samples were excluded from the Hen-1 and GSE20388 datasets.

RNA-Seq

Other studies used RNA-Seq to quantify gene expression. To do this, sequencing adaptors were ligated to both ends of the cDNA fragments (X. Wang, 2016). The sequencing adaptors allowed for detection by the sequencer and also permitted sequencing of multiple samples at the same time, since different samples had distinct adapters, preventing interference between the samples (X. Wang, 2016).

Following cDNA library construction, the cDNA was sequenced. The studies within our meta-analysis employed one of two RNA sequencing platforms: either Illumina HiSeq 2000 or the Illumina NextSeq 500 platforms *(see Appendix 1 for study-specific details)*. Within both of these platforms, the cDNA fragments were lined up inside the sequencer vertically in a grid-like pattern. Each base pair was assigned a fluorescent probe that bound to the cDNA fragments one base pair at a time, beginning at the bottom end of the vertical sequence. The machine then took a top view picture each time a probe bound to a base pair. The base pair was identified based on the color fluorescing in that picture. The machine then washed the color off of the probes after each picture was taken, and repeated this process until the complete sequence had been determined (X. Wang, 2016).

The studies included in our meta-analysis used either 50, 75, or 100 single-end bp (base pair) reads or 100 bp paired-end reads. In single-end reading, the cDNA fragment was read only from one end to another, while paired-end reading occurred at both ends, forming read pairs (X. Wang, 2016). By doubling the total number of sequence reads, paired sequencing facilitated the later step of alignment to the reference genome (X. Wang, 2016).

RNA-Seq Data Preprocessing

Having determined the sequences of the cDNA from the sample, we ran each experiment within the HDRF Data Center through the same quality control (QC) and annotation pipeline. We ran the RNA-Seq data through QC using fastp (v.0.20.1, default parameters), a preprocessing tool that, based on a number of QC metrics, quickly performs read filtering and pruning, adapter

trimming, base correction, and default data exclusion to improve the quality of the data collected. Base correction ensured that the chance of seeing each of the four bases at each base position was the same, otherwise there may have been a problem in the library construction process or non-random fragmentation (X. Wang, 2016, p. 20).

The next step of RNA-Seq analysis was to count the number of reads representing transcripts generated from different regions of the genome to quantify gene expression (X. Wang, 2016). The process of determining where these reads map onto the genome is called aligning the sequencing data to the genome (X. Wang, 2016). We performed read mapping (or alignment) using the sequencing algorithm STAR (v.2.7.4a, default parameters except for outSAMattributes= "NH AS NM MD XS" and outSAMstrandField= "intronMotif"). The genome build used for this alignment was *Mus musculus* GRCm38 and *Rattus norvegicus* Rnor6.0, referencing ENSEMBL 98 genome annotation (Version 3.52.2). This algorithm implemented the *ab initio* method, which is the Latin phrase, "from the beginning" (X. Wang, 2016). This method solves the problem posed by alternative splicing that makes it difficult to continuously map reads due to spliced introns (X. Wang, 2016). It detected splice junctions by using parts of the reads to map, and then extending candidate hits. In this way, reads mapping was not dependent on the current gene exonic annotation of the reference genome (X. Wang, 2016).

The aggregate amount of reads aligning to locations of the genome representing genes ("counts") was assessed to determine the presence and extent of gene expression. We performed this quantification of the reads that mapped onto the genome using the subread R package (featureCounts v.2.0.1, default parameters). Within the RNA-Seq data, no samples were excluded beyond those excluded during quality control in the analysis for the original publications. Finally, the gene symbols representing those genes were provided as annotation (X. Wang, 2016). At this point, the data was ready for downstream analysis.

Differential Expression Analysis

By comparing the gene expression profiles of two or more samples, we can illuminate an inventory of differences between groups. Despite the differences among the two transcriptional profiling methods incorporated in this meta-analysis, the preprocessed data were in a similar

format. This allowed for similar differential expression analysis for the output of both microarray and RNA-Seq datasets (Malone & Oliver, 2011).

We ran the differential expression analysis in R using the limma package to fit a linear model to each gene (v.3.52.2). Limma stands for "Linear Models for Microarray data" (Ritchie et al., 2015), but, contrary to the name, limma is used for differential gene expression analysis of microarray, PCR, and RNA-seq data, and is particularly useful for overcoming small sample sizes (Ritchie et al., 2015). However, RNA-Seq and microarray output are two distinct forms of data: the former is discrete, while the latter is continuous (Ritchie et al., 2015). This introduced an additional step in data analysis to ensure comparability across the studies. To solve this discrepancy, the function "voom" was used for variance stabilization for the RNA-Seq data prior to differential expression analysis (Ritchie et al., 2015). The linear model for each experiment was set so that all experimental subgroups and brain regions were included in the omnibus model, but then contrasts for each relevant subgroup comparison was outputted for each brain region (Ritchie et al., 2015). The t-statistics outputted from these contrasts were then moderated using an empirical Bayes correction (function *ebayes()* within the *limma* package) (Ritchie et al., 2015).

Effect Size Calculation

From the differential expression analysis output, we calculated an effect size for each gene - a standardized value representing the difference between the two groups (Sullivan & Feinn, 2012). The sampling variance of the effect size was used to establish confidence intervals (Lakens, 2013). Sampling variance depends on the sample size (Lakens, 2013). Generally speaking, the larger the sample size, the smaller the variance. There are many options for effect sizes: the statistic used for this meta-analysis was Hedge's *g*, which is a standardized mean difference statistic (Lakens, 2013). We calculated the Hedge's *g* for each gene of each study based on the moderated t-statistic. This t-statistic was obtained through a differential expression analysis conducted within the *limma* pipeline for microarray, or *limma-voom* pipeline for RNA-Seq. The effect sizes and variances were calculated without use of a code package.

Preparing for Meta-Analysis: Aligning the Results of Different Datasets

Since each dataset presents a slightly different list of genes included in the output result, this necessitates a process termed alignment across datasets, or the merging of dataset information for each gene (X. Wang, 2016). We first aligned gene expression profiles for genes with the identical ENSEMBL gene ID from within the same species. Then, we took the combined gene expression profile for mice and the combined gene expression profile for rats and aligned those lists based on genes with identical gene symbols. However, gene symbols commonly differ in different species. To deal with this problem, we used a list of gene orthologs from the ENSEMBL website (https://useast.ensembl.org/info/data/biomart/biomart_combining_species_datasets.html). Gene orthologs are defined as a type of homologous gene that come from a common ancestral gene and encode proteins that carry out identical functions in different species (Koonin, 2005).

After combining datasets, the number of genes common between them was a smaller subset when compared to the study profiles individually. In order for a gene to be included in the meta-analysis, we required 75% of all group comparisons in the meta-analysis to include that gene. In the final aligned dataset, we had a total of 14,770 genes.

Meta-Analysis Procedure

We performed a meta-analysis of the effect sizes using the method of inverse variance in the function *rma()* in the R package Metafor (v3.8-1, default parameters). Multiple comparisons correction was performed using the Benjamini-Hochberg method, which is also called a False Discovery Rate correction (FDR). FDR is an important statistical consideration when conducting multiple comparisons due to the increased probability of false positive results, meaning that a result is incorrectly determined to be unlikely to occur under conditions of random chance. By taking a ratio of the positive results within our study compared to the number false positives likely to occur based on the number of statistical comparisons that we are conducting, and adjusting the p-value accordingly, we are able to concurrently identify as many significant results as possible while minimizing the proportion of false positives.

We then visualized many of our top results from the meta-analysis using forest plots. Forest plots graphically represent effect sizes and their associated confidence intervals across multiple studies. They also display the estimated common effect and confidence interval from

the meta-analysis output. They can be used to determine whether the meta-analysis results may be influenced by an outlier, or which particular studies might be driving the common effect compared to others.

Interpreting Meta-Analysis Output: Downstream Analyses

Overview

Based on the meta-analysis results, genes that were differentially expressed in our meta-analysis with an FDR <0.1 were investigated using the public database DropViz to understand the cell type and regional specificity of their expression in the brain (Saunders et al., 2018; Szklarczyk et al., 2015). Then we used Gene Set Enrichment Analysis (fGSEA) to determine whether the overall pattern of differential expression associated with our depression models was enriched for effects within gene sets representing particular functional, anatomical, and cell-type categories.

Cross-referencing differentially expressed genes with cell type database DropViz

Our meta-analysis used bulk dissection samples, and therefore measured the average gene expression across all cell populations for a brain region. In contrast, single-cell RNA-Seq (scRNA-Seq) experiments profile individual cells to find molecular distinctions linked only to specific cell types. To obtain information regarding the brain cell types typically expressing each of our differentially expressed genes, we used the DropViz scRNA-Seq atlas. The DropViz database is derived from a study that sampled from late adolescent/adult (P60-P70) male C57Blk6/N mice and used Drop-seq to profile single-cell RNA expression from nine brain regions, including the hippocampus (Saunders et al., 2018). The sequenced cells were then grouped into eight broad classes (neurons, astrocytes, microglia/macrophages, oligodendrocytes, polydendrocytes, and components of the vasculature—endothelial cells, fibroblast-like cells, and mural cells), based on an independent component analysis of the scRNA-Seq data and known cell type markers.

To use DropViz, we entered our DE gene list into the gene search tools on their websites. Since the DropViz atlas was derived from mice, we used the mouse orthologs for the gene symbols for our DE genes. We then downloaded their relative expression within different

hippocampal cell types under basal conditions. High expression of a majority of the DE genes in particular cell types could reveal potential biological targets in depression.

Functional Ontology

We evaluated whether our differential expression results were enriched for genes representing particular functional, anatomical, and cell-type categories using fGSEA (Sergushichev, 2016) (v.1.2.1, nperm=50,000, minSize = 10, maxSize = 1000) and a previously constructed, custom gene set file ("Brain.GMT", # of gene sets: 15914, see *Appendix 2*) containing gene sets related to brain cell types, regions, processes, and experimental results, as well as more standard functional ontology. To run the analysis, we used meta-analysis results that were annotated by official rat gene symbol (or rat ortholog) and pre-ranked by the meta-analysis estimate (estimated Hedge's g), with any results that mapped to the same gene symbol averaged to produce 14,332 rows of input.

Results

We ran a meta-analysis of the results from ten hippocampal transcriptional profiling studies generated across five animal models of depression used within HDRF-associated laboratories to find convergent differential expression. This meta-analysis including thirteen separate statistical comparisons of depression models and control animals. We predicted that the animal models of depression would collectively produce converging, significant differences in gene expression compared to controls, and might reveal additional genes that had not been found to be significantly differentially expressed within each study's original individual analysis.

Differentially Expressed Genes (DEGs): Similarities and Differences Across Models

Out of a total of 14,770 genes, the meta-analysis revealed fifteen DEGs with FDR<0.05 and twenty-seven DEGs with FDR<0.10 (**Table 4**), despite differences in species, platform, and tissue extraction procedures indicated in **Table 2**. The volcano plot of the meta-analysis results (FDR<0.05) displays a large negative skew with only one gene (Arl16) with a positive estimate, indicating that the most significant genes were downregulated by the experimental manipulation (**Figure 1**).

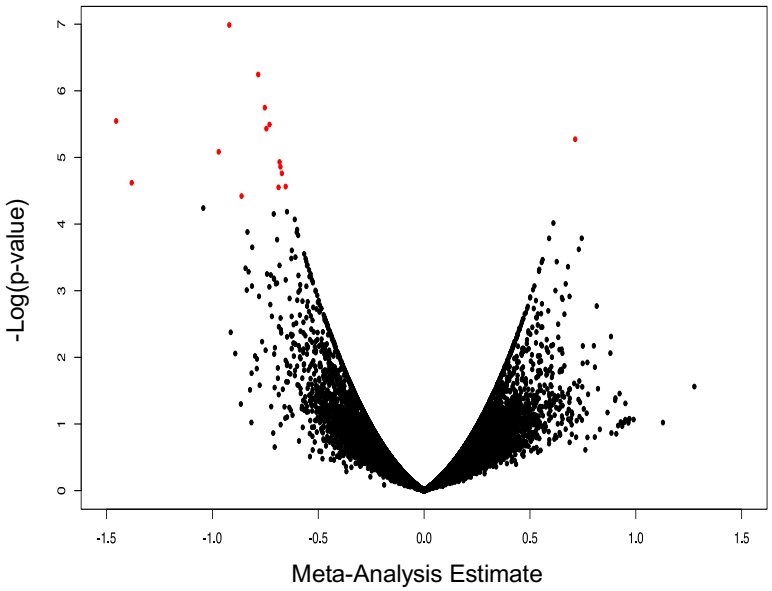

Figure 1. Volcano Plot of Hippocampal Meta-Analysis Differentially Expressed Genes

The meta-analysis estimate is plotted against the inverse of the log10 p-value for the result (-Log(p-value)). A meta-analysis estimate unit of 1 is the estimated effect size across models (Hedge's G), which is approximately the group difference divided by the standard deviation. Higher values on the y-axis indicate greater statistical significance (smaller p-value). The red dots indicate the 15 DEGs with an FDR <0.05.

Symbol	Estimate	SE	Pvalue	FDR
Slc27a1	-9.20E-01	1.73E-01	1.03E-07	1.51E-03
Pamr1	-7.84E-01	1.57E-01	5.70E-07	4.21E-03
Aloxe3	-7.53E-01	1.58E-01	1.79E-06	8.80E-03
Ephx2	-1.45E+00	3.11E-01	2.84E-06	9.10E-03
Acsbg1	-7.30E-01	1.57E-01	3.21E-06	9.10E-03
Sox6	-7.45E-01	1.61E-01	3.70E-06	9.10E-03
Arl16	7.14E-01	1.57E-01	5.33E-06	1.12E-02
Slc15a2	-9.70E-01	2.18E-01	8.23E-06	1.52E-02
Dpy19l1	-6.83E-01	1.56E-01	1.17E-05	1.92E-02
Maob	-6.79E-01	1.56E-01	1.38E-05	2.04E-02
Gramd3	-6.72E-01	1.56E-01	1.73E-05	2.33E-02
Phgdh	-1.38E+00	3.27E-01	2.40E-05	2.96E-02
Ntm	-6.54E-01	1.56E-01	2.74E-05	2.96E-02
Slc1a3	-6.88E-01	1.64E-01	2.81E-05	2.96E-02
Mfge8	-8.63E-01	2.09E-01	3.80E-05	3.74E-02
Fcrls	-1.04E+00	2.59E-01	5.75E-05	5.31E-02
Mlc1	-6.48E-01	1.62E-01	6.52E-05	5.66E-02
Gnb3	-7.10E-01	1.79E-01	7.05E-05	5.79E-02
Sall1	-6.11E-01	1.56E-01	8.52E-05	6.62E-02
C3	6.11E-01	1.57E-01	9.65E-05	7.13E-02
Plcd1	-6.00E-01	1.56E-01	1.21E-04	8.51E-02
Krt80	-8.35E-01	2.18E-01	1.31E-04	8.55E-02
Scg3	-6.02E-01	1.58E-01	1.33E-04	8.55E-02
Grm3	-5.95E-01	1.57E-01	1.47E-04	9.07E-02
Nrip3	7.44E-01	1.97E-01	1.63E-04	9.31E-02
Calm3	5.91E-01	1.57E-01	1.64E-04	9.31E-02
Slc39a12	-6.94E-01	1.85E-01	1.71E-04	9.36E-02

Table 4. List of the top 27 DE genes (FDR<0.10).

List of the top 27 DE genes with meta-analysis estimate, SE (standard error) and FDR (False Discovery Rate). The only significant DE genes with a positive meta-analysis estimate is Arl16 and C3, and the rest have a negative estimate. Genes are listed from lowest to highest FDR, with a cutoff of FDR<0.10.

We created forest plots for each DE gene to deconstruct the summary meta-analysis estimates and observe the individual effect sizes for each comparison. These example forest plots shown below provide information on both the quantitative (how extreme) and qualitative (which direction) heterogeneity across models. In **Figure 2**, we provide examples of forest plots illustrating Pamr1 and Ephx2 differential expression, which have consistent down-regulation across almost all models. In general, we found that some of the forest plots showed clustering of

models into two categories: selective breeding models (bHR-bLR and FSL-FRL) vs. CORT or stress manipulation models. For example, for Ephx2 (**Figure 2B**), there is a slightly stronger effect in genetic models. This led us to create a hierarchically-clustered heatmap of DE genes by dataset to confirm this pattern of heterogeneity and group effects (**Figure 3**).

A

Pamr1

Comparison	Model	Name	Region	Estimate	P-value
Susceptible - Control	CSDS	Nestler-3	vHPC	0.44	0.61192
bLR - bHR	bHR-bLR	Akil-6	HPC	-0.21	0.73044
Susceptible - Control	CSDS	Meaney-2	vDG	-0.38	0.23230
Susceptible.Saline - Control.Saline	CSDS	Nestler-1	vHPC	-0.44	0.56014
GRov - WT	GRov	Akil-1	HPC	-0.51	0.39744
FSL - FRL	FSL	McEwen-4	vDG	-0.83	0.29735
FSL - FRL	FSL	GSE20388	HPC	-0.89	0.00669
Susceptible - Control	CSDS	Nestler-3	vHPC	-1.16	0.10080
Susceptible - Control	CSDS	Nestler-3	vHPC	-1.18	0.14901
bLR - bHR	bHR-bLR	Akil-5	HPC	-1.19	0.04507
CORT.WT - Saline.WT	Cort	McEwen-5	vHPC	-1.35	0.14092
EL.GRov - Control	GRov	Akil-4	DG	-1.49	0.01159
LT.GRov - Control	GRov	Akil-4	DG	-1.58	0.00774
Summary				-0.78	5.7e-07

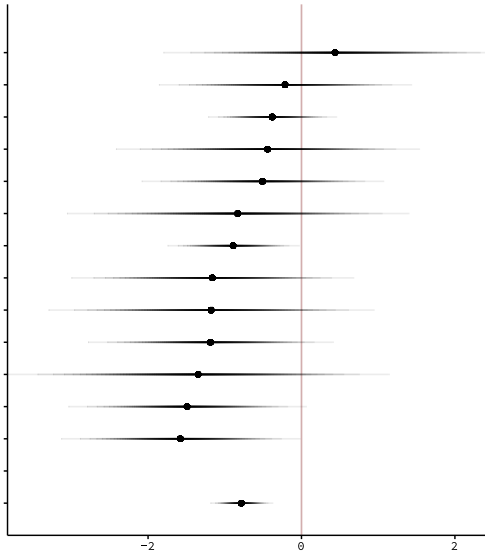

B

Ephx2

Comparison	Model	Name	Region	Estimate	P-value
Susceptible - Control	CSDS	Nestler-3	vHPC	-0.30	7.26e-01
Susceptible - Control	CSDS	Meaney-2	vDG	-0.34	2.87e-01
Susceptible - Control	CSDS	Nestler-3	vHPC	-0.43	5.38e-01
Susceptible.Saline - Control.Saline	CSDS	Nestler-1	vHPC	-0.56	4.63e-01
GRov - WT	GRov	Akil-1	HPC	-0.84	1.64e-01
Susceptible - Control	CSDS	Nestler-3	vHPC	-1.19	1.46e-01
EL.GRov - Control	GRov	Akil-4	DG	-1.36	2.04e-02
LT.GRov - Control	GRov	Akil-4	DG	-1.38	1.88e-02
CORT.WT - Saline.WT	Cort	McEwen-5	vHPC	-1.76	5.87e-02
bLR - bHR	bHR-bLR	Akil-5	HPC	-2.15	1.23e-03
bLR - bHR	bHR-bLR	Akil-6	HPC	-2.25	1.02e-03
FSL - FRL	FSL	GSE20388	HPC	-3.27	3.64e-16
FSL - FRL	FSL	McEwen-4	vDG	-4.47	9.52e-05
Summary				-1.5	2.84e-06

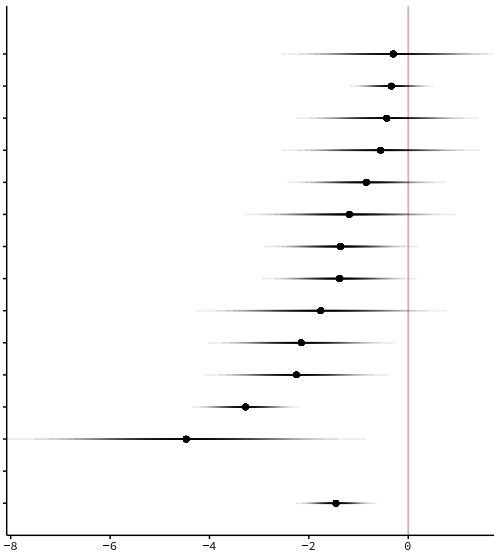

Figure 2. Example Forest Plots Illustrate Model Similarity and Heterogeneity in Effects on Hippocampal Differential Expression.

Figure 2A&B. Top DE Gene Forest Plots. The comparison on the left side of the chart corresponds to the horizontal line in the forest plot. The center of the line, indicated by the black dot, is the effect size (Hedge's G) for the group comparisons from each individual study or the collective estimated effect size from the meta-analysis. The width of the line 95% confidence

intervals. The group comparisons from the individual studies are ordered by effect size, from smallest to largest. Information about the model, dataset name, brain region, and p-value are also indicated. The abbreviated brain regions are: vHPC (ventral hippocampus), HPC (hippocampus), vDG (ventral dentate gyrus) DG (dentate gyrus).

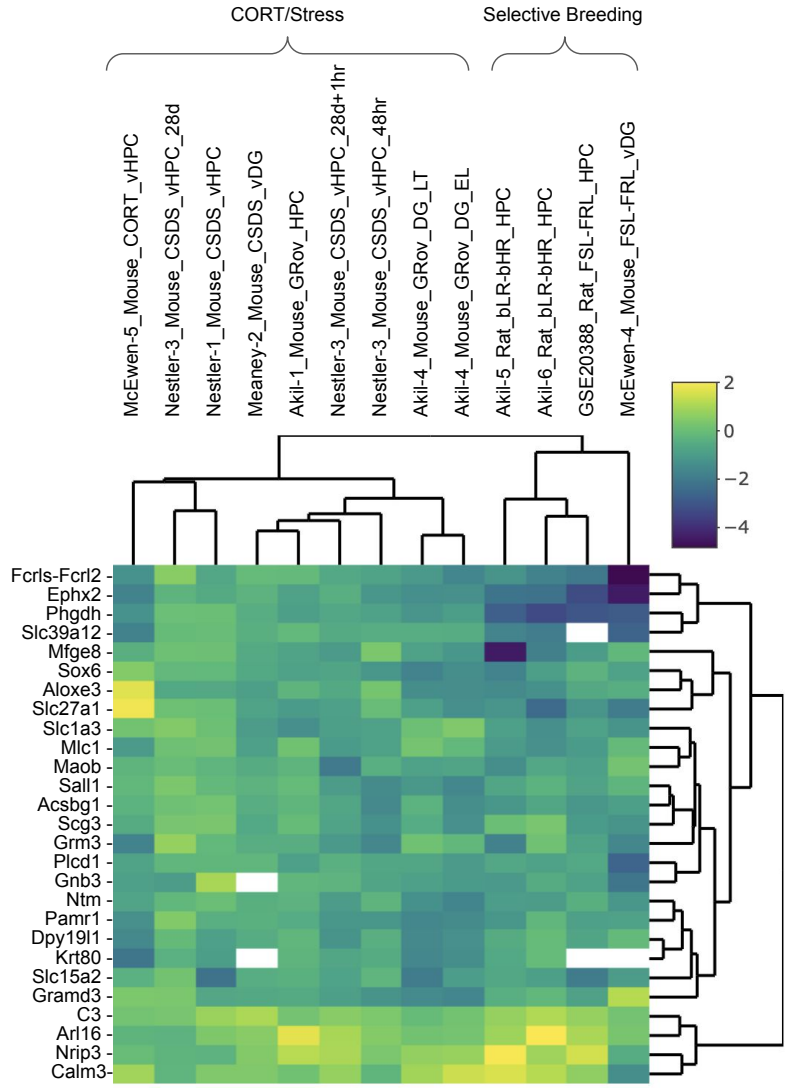

Figure 3. Meta-analysis Demonstrates Model Heterogeneity via Distinctly Grouped Effects on Hippocampal Differential Expression.

A hierarchically clustered heatmap produced with the top meta-analysis genes (FDR<0.1) shows similar depression models clustering together, with datasets related to stress/glucocorticoids on the left and datasets related to genetic predisposition for internalizing behavior on the

right. Heatmap cells are color coded by meta-analysis estimated effect size (Hedge's G), with yellow indicating a positive estimate and a dark blue indicating a negative estimate.

Functional Patterns in the Results

Next, we analyzed the functional patterns present in the hippocampal depression model meta-analysis output using Fast Gene Set Enrichment Analysis (fGSEA) and a custom database of gene sets related to functional pathways, stress, psychiatric illness, behavior, and cell type ("Brain.GMT"). Using fGSEA, we examined the enrichment of down-regulation or up-regulation in our meta-analysis results within previously defined gene sets. In other words, fGSEA provided a statistical determination of whether a particular gene set showed more upregulation or downregulation than would be expected by random chance. The statistical significance was determined using 50,000 permutations. Of the 10,261 gene sets included in the final fGSEA output, nineteen were derived directly from the depression model results from the original studies included in our meta-analysis and were excluded from further consideration due to circularity. Of the remaining 10,242 gene sets, 447 had an FDR<0.05 and 193 had FDR<0.01 (1.9% of all relevant gene sets). The most highly significant gene sets were skewed towards upregulation: out of the 193 gene sets with FDR<0.01, 113 were upregulated and 80 were down-regulated.

Overall, we found downregulation in sets of genes with enriched expression in glial cell types, including astrocytes, ependyma, oligodendrocytes, and polydendrocytes. Of the 80 down-regulated gene sets with FDR<0.01, 69% (55/80) were explicitly related to cell type, particularly astrocytes, oligodendrocytes, endothelial cells, ependymal cells, and epithelial cells, as well as a few neuronal subtypes. When ranked by smallest Normalized Enrichment Score (NES), or most down-regulated, we observed that all of the top ten down-regulated gene sets were related to cell type: gene sets ranked #1-5 were all related to astrocytes, whereas gene sets ranked #6-10 included other cell types, including oligodendrocytes, interneurons, and a subtype of neuron in the subiculum (DropViz_HC_Neuron_Subiculum_Slc17a6_cluster-markers.csv). The down-regulated results also included five hippocampal co-expression networks.

Of the 113 upregulated gene sets with FDR<0.01, we noted 12% (14/113) related to cell type, especially neurons and microglia. Ranking the top ten gene sets by highest NES, three of

these (ranked 2, 4, and 7) fell into this category. Within the gene sets more selectively defined by having highly enriched expression in particular hippocampal cell types (**Figure 4**), the CA1 pyramidal neurons stood out as the only gene set with significant upregulation (FDR<0.05, Figure 4). Four of the top upregulated gene sets were related to hippocampal co-expression networks, one of which was ranked #8 by NES. There were also functional themes: 10% (11/113) of the gene sets were related to RNA transport or processing, and another seven gene sets were related to immunity, inflammation, or autophagy, including the most upregulated gene set.

In general, we saw strong enrichment of both upregulated and downregulated gene sets related to the etiology or symptomology of depression, as derived from ontology databases or more directly from the results from other transcriptional profiling studies. Overall, 108 gene sets were related to stress or mood, of which 9.3% (10/108) showed strong enrichment (FDR<0.01) for differential expression in our meta-analysis. This is five times greater than the rate of strong enrichment (FDR<0.01) in non-mood gene sets (9.3% in mood/stress gene sets /1.8% in non-mood/stress gene sets). Therefore, gene sets related to stress or mood were five times more likely to be enriched for differential expression in our meta-analysis.

Cell Type	FDR	NES
Astrocyte_Gja1 (DropViz: Hippocampus)	3.49E-03	-3.25
Astrocytes (Cahoy 2008)	3.49E-03	-2.86
Astrocytes (Darmanis 2015)	3.49E-03	-2.32
Astrocytes (Zeisel 2015)	3.49E-03	-2.45
Astrocytes (Zhang 2014)	3.49E-03	-2.16
Polydendrocyte_Tnr (DropViz: Hippocampus)	3.49E-03	-2.51
Oligodendrocyte Progenitors (Darmanis 2015)	6.19E-01	-1.16
Oligodendrocyte Progenitors (Zhang 2014)	3.34E-01	-1.41
Oligodendrocytes_Newly-Formed (Zhang 2014)	6.27E-01	-1.13
Oligodendrocyte_Tfr (DropViz: Hippocampus)	3.49E-03	-2.54
Oligodendrocytes (Cahoy 2008)	1.52E-02	-1.99
Oligodendrocytes (Darmanis 2015)	4.69E-01	-1.30
Oligodendrocytes (Zeisel 2015)	5.44E-03	-1.60
Oligodendrocytes_Myelinating (Zhang 2014)	5.04E-01	-1.24
ChoroidPlexus_Ttr (DropViz: Hippocampus)	2.12E-02	-1.76
Ependyma (DropViz: Hippocampus)	3.49E-03	-1.85
Neurogenesis_Sox4 (DropViz: Hippocampus)	9.14E-01	-0.80
FibroblastLike_Dcn (DropViz: Hippocampus)	6.42E-02	-1.54
Endothelial_Flt1 (DropViz: Hippocampus)	9.43E-01	0.86
Endothelial Cells (Darmanis 2015)	3.00E-01	-1.49
Endothelial Cells (Zeisel 2015)	8.85E-01	0.92
Endothelial Cells (Zhang 2014)	6.05E-01	1.15
Endothelial Cells (Daneman 2010)	9.83E-01	0.64
Mural_Rgs5Acta2 (DropViz: Hippocampus)	7.34E-02	-1.51
Mural Cells (Zeisel 2015)	9.62E-01	-0.79
Pericytes (Zhang 2014)	9.95E-01	-0.59
Vascular Cells (Daneman 2010)	6.85E-02	-1.73
Microglia_Macrophage_C1qb (DropViz: Hippocampus)	3.67E-01	-1.22
Microglia (Zeisel 2015)	9.73E-01	0.84
Microglia (Darmanis 2015)	5.13E-01	1.27
Microglia (Zhang 2014)	7.19E-01	-1.03
Neurons (Cahoy 2008)	6.55E-01	-1.08
Neurons (Darmanis 2015)	7.79E-01	0.95
Neurons (Zhang 2014)	7.73E-01	-0.97
Pyramidal Neurons (Zeisel 2015)	8.44E-03	-1.74
CA1 Pyramidal Neurons (Zeisel 2015)	3.49E-03	2.16
Interneurons (Zeisel 2015)	5.99E-02	-1.42
Interneuron_Gad2 (DropViz: Hippocampus)	3.49E-03	-2.51
Neuron_CajalRetzius_Lhx1 (DropViz: Hippocampus)	2.45E-01	-1.47
Neuron_Subiculum_Slc17a6 (DropViz: Hippocampus)	3.49E-03	-2.67

Figure 4. Enrichment of Differential Expression Identified in our Meta-analysis of HDRF Depression Models in Glial Cell Type Gene Sets.

Gene sets with enriched expression in glial cell types, including astrocytes, ependyma, choroid plexus cells, oligodendrocytes, polydendrocytes and interneurons all show downregulation using fGSEA analysis. Gene sets are grouped by cell type. Similar to Figure 2, the yellow to blue gradient of normalized enrichment scores (NES) indicate the range of positive (upregulated) to negative (downregulated) NES scores, respectively. A low false detection rate (FDR) is

highlighted in purple. The names of cell types which survived false discovery correction are in purple to help distinguish the statistically significant results (FDR<0.05).

To further investigate our glial cell type findings within the fGSEA results, we cross-referenced our top DEGs with the online database DropViz. This database possesses single cell RNA-Seq data comparing gene expression in different cell types under basal conditions in the adult mouse brain (Saunders et al., 2018). Inputting the top DEGs from this meta-analysis, as well as indicating the brain region (HPC), revealed that the top DEGs show highest expression in the hippocampus in glial cell types, particularly astrocytes, under basal conditions (**Figure 5**).

Gene	Meta-Analysis Estimate	Oligodendrocyte	Astrocyte	Ependyma	Choroid Plexus	Fibroblast-Like	Mural	Microglia_Macrophage	Endothelial	Polydendrocyte	Neurogenesis	Neuron_CajalRetzius	Interneuron	Neuron_Subiculum	Neuron_Subiculum_EC	Neuron_Dentate	Neuron_CA1	Neuron_CA2CA3
Ephx2	-1.45	0.19	3.09	4.47	3.82	2.37	2.70	1.70	0.39	1.92	2.31	0.14	0.49	0.54	0.47	0.22	0.27	0.34
Phgdh	-1.38	0.47	11.89	1.59	4.09	2.49	0.94	0.57	0.11	0.36	0.46	0.27	0.72	0.16	0.37	0.34	0.56	0.42
Fcrls	-1.04	4.56	115.24	87.85	0.55	2.61	2.26	3.40	1.49	2.20	6.08	2.33	0.98	1.06	1.04	0.91	0.85	0.66
Slc15a2	-0.97	8.34	87.90	6.99	1.64	28.24	6.33	9.43	4.19	29.23	6.85	20.72	81.69	91.18	49.16	8.70	72.32	6.79
Slc27a1	-0.92	3.07	32.99	10.64	4.36	2.61	0.69	1.79	0.99	2.28	2.46	2.88	1.04	1.40	1.40	1.31	1.14	0.87
Mfge8	-0.86	0.47	0.26	0.10	0.27	1.78	1.07	195.74	0.42	0.76	2.69	0.41	0.13	0.14	0.12	0.17	0.18	0.11
Pamr1	-0.78	1.09	24.46	9.77	2.18	1.07	0.88	3.49	0.47	2.16	1.92	0.41	0.25	0.28	0.23	0.47	0.26	0.64
Sox6	-0.75	0.50	5.76	6.01	0.00	0.00	4.58	0.66	0.24	21.02	3.92	0.27	2.01	0.10	0.08	0.09	0.10	0.07
Aloxe3	-0.75	21.97	670.82	75.36	3.00	73.10	12.10	28.58	8.79	26.14	43.62	13.03	5.28	6.11	4.42	5.64	4.56	3.32
Acsbg1	-0.73	0.19	4.57	26.37	0.27	2.97	0.13	0.38	0.19	0.96	0.08	1.92	0.34	2.03	6.95	0.10	0.13	0.07
Gnb3	-0.71	16.15	28.09	0.87	0.27	0.47	4.01	0.94	0.37	0.72	1.15	0.82	0.64	5.60	8.33	0.70	1.78	0.23
Slc39a12	-0.69	2.18	2.50	2.78	2.18	3.68	2.70	2.45	3.30	3.44	4.00	4.12	4.58	4.07	4.92	5.69	4.38	5.01
Slc1a3	-0.69	4.04	8.37	3.39	1.09	3.20	1.63	0.28	0.44	6.09	0.08	0.14	0.07	0.07	0.09	0.10	0.08	0.07
Dpy19l1	-0.68	6.99	197.81	4.78	26.18	12.58	198.04	7.08	13.02	18.02	36.77	4.53	1.62	1.88	3.09	1.82	1.41	1.02
Maob	-0.68	2.06	2.90	3.75	0.00	5.93	0.75	29.62	0.06	1.76	1.62	0.14	1.30	0.06	0.10	0.08	0.05	0.06
Gramd3	-0.67	0.11	0.06	0.41	0.00	0.12	0.13	0.19	0.03	0.04	0.38	0.14	0.22	1.50	1.40	1.16	0.71	0.44
Mlc1	-0.65	18.55	326.23	84.77	1.36	6.76	7.21	11.98	5.59	32.95	43.54	75.32	42.53	28.04	32.50	14.38	20.18	15.24
Ntm	-0.65	2.97	23.67	11.87	65.45	3.09	1.25	0.28	8.29	0.80	1.15	2.61	0.38	0.37	1.92	0.24	0.42	0.32
Sall1	-0.61	2.94	76.72	1.64	0.27	1.90	1.44	2.45	1.05	2.00	2.85	2.88	0.62	0.75	0.72	0.62	0.60	0.39
Scg3	-0.60	1.18	38.25	10.80	23.18	1.07	0.56	1.70	0.65	0.20	0.08	0.82	0.22	0.34	0.24	0.27	0.41	0.45
Grm3	-0.60	3.14	1.97	0.98	1.09	3.09	3.70	5.47	2.28	2.72	3.54	3.43	52.68	2.63	17.77	10.63	25.73	75.51
Plcd1	-0.60	0.01	0.01	0.00	0.00	0.00	0.00	0.00	0.00	0.00	0.00	0.00	0.01	0.01	0.00	0.00	0.01	0.00
Calm3	0.59	0.00	0.05	4.58	0.00	0.00	0.00	0.00	0.06	0.12	0.00	0.00	0.03	0.00	0.01	0.00	0.00	0.01
C3	0.61	17.64	22.60	2.36	4.36	0.71	0.19	4.34	0.29	3.20	4.08	0.69	0.23	0.60	0.16	0.85	0.18	0.10
Arl16	0.71	21.68	2.48	7.81	2.18	3.68	1.38	6.79	5.46	8.69	2.77	7.96	8.60	17.36	11.04	2.94	8.02	1.05
Nrip3	0.74	44.24	46.01	75.41	53.18	40.82	55.29	28.58	26.53	38.91	71.85	66.13	107.81	127.48	89.56	123.47	138.56	166.43

Figure 5. The Top Differentially Expressed Genes Identified by Our Meta-Analysis of Depression Models Are Most Highly Expressed in Astrocytes Under Basal Conditions

Using Single Cell RNA-Seq data from the DropViz database, we find that the top DEGs from our meta-analysis are most highly expressed under basal conditions in glial cell types, with the strongest expression in astrocytes. The DEGs (FDR<0.1) are sorted by meta-analysis estimate (Hedge's G, left column, blue-yellow color scale described previously). The cell types with high relative expression of each gene are shown in darker green, relative to the expression for that gene overall across cell types. The DE gene Krt80 was excluded due to the lack of data in DropViz. The abbreviated cell type names from the DropViz database are listed from left to right: Oligodendrocyte_Tfr [#8], Astrocyte_Gja1 [#7], Ependyma [#11], Choroid_Plexus_Ttr [#12], Fibroblast-Like_Dcn [#17], Mural_Rgs5Acta2 [#16], Microglia_Macrophage_C1qb [#10], Endothelial_Flt1 [#15], Polydendrocyte_Tnr [#9], Neurogenesis_Sox4 [#13], Neuron_CajalRetzius_Lhx1 [#14], Interneuron_Gad2 [#1], Neuron_Subiculum_Slc17a6 [#2], Neuron_Subiculum_Entorhinal_Nxph3 [#3], Neuron_Dentate_C1ql2 [#4], Neuron_CA1_Subiculum_Postsubiculum_Entorhinal_Fibcd1-Dcn-Cbln1-Ptgfr-Fezf2 [#5], Neuron_CA2CA3_Pvrl3-Rgs15-Calb2 [#6]

Discussion

The Hope for Depression Research Foundation brings together five laboratories that conduct transcriptomic studies using a variety of animal models of depression. In this study, to better understand the neurobiology of depression, we integrated results across HDRF models in an effort to identify unifying trends. To do this, we used a meta-analysis pipeline to extract consistent hippocampal gene expression signatures. We incorporated a total of five animal models: two models of genetic predisposition for internalizing behavior (FSL/FRL rats, and bLR/bHR rats) and three related to stress susceptibility or altered stress physiology (CORT mice, CSDS mice, and GRov mice). The transcriptomic data (microarray or RNA-Seq) represented gene expression within the hippocampus or dentate gyrus. We used the HDRF Gene Explorer to run a multi-level, random effects meta-analysis model of thirteen depression-control comparisons and found twenty-seven candidate genes (FDR<0.10) despite the initial appearance of minimal intersection among top results from each study.

Notably, many of the genes that we identified with consistent differential expression across models of depression had previously been recognized for involvement in psychiatric

illnesses, including depression. Our differential expression results contained genes previously recognized for involvement in neuroimmunity (neuroinflammation and phagocytosis), and cell proliferation and migration. We also identified striking functional and cell-type expression patterns in the meta-analysis differential expression output. Under basal conditions, many of our top DEGs are preferentially expressed in astrocytes or other non-neuronal cell types, including ependyma, choroid plexus cells, oligodendrocytes, and polydendrocytes. As we will discuss below, this downregulation of astrocyte-related gene expression within our depression models mirrors results from post-mortem MDD patients indicating reduced hippocampal astrocyte-related gene expression (Medina et al., 2016). This finding demonstrates the utility of combining results from diverse models to achieve an improved understanding of the neurobiology of depression.

Functional Themes: The Role of Astrocyte-related Gene Expression in Depression

Many of our top differentially expressed genes are involved in the function of astrocytes and other glial cells, as well as in cell proliferation, migration, and neurodevelopment. The prevalence of astrocyte-related genes in our results fits with an increasing body of evidence from both preclinical and clinical studies that have implicated glial dysregulation in the pathology of mood disorders. In human post-mortem studies, MDD brains have decreased density and/or fewer astrocytes by cell count (Hu et al., 2019). Downregulation of astrocyte-related gene expression is also observed in depressed individuals (Medina et al., 2016). Hippocampal microarray profiles from human post-mortem brains with MDD show downregulation of key astrocyte-related genes, specifically those involved in the syncytial maintenance of homeostasis by astrocytes (potassium and water transporters, gap junction proteins, and glutamate transporters), including one of our top DEGs, SLC1A3 (Hagenauer et al., 2018; Medina et al., 2016). Downregulation of these genes is suggested to disrupt the glial network, leading to imbalanced glutamatergic synaptic activity in patients with MDD (Medina et al., 2016). This is consistent with our findings that genes that are both highly expressed in astrocytes and affect glutamatergic signaling are downregulated in animal models of depression.

Downregulation of astrocytic genes is found in other animal models of depression as well. For example, the chronic unpredictable stress model bears 19% fewer astrocytes (Banasr & Duman, 2008). Astrocytes have also been a target of animal depression models. Astrocyte-

selective ablation in the prefrontal cortex of rats induced depressive-like behaviors measured by four behavioral batteries (Banasr & Duman, 2008). These effects were not found in rats treated with a neurotoxin in the same brain region, suggesting that glial loss, not neuronal loss, could contribute to symptoms of anhedonia, anxiety, and helplessness (Banasr & Duman, 2008). Additionally, the gliotoxin used in the previous study (L-alpha-aminoadipic acid) to generate the depressive-like phenotype inhibited both glutamate transport and glutamine synthetase, aspects of glutamatergic signaling supported by the syncytial functions of astrocytes (Medina et al., 2016). These results therefore also reinforce the glutamatergic system as a target for treatment resistant depression, as well as the importance of astrocytes for this system (Banasr & Duman, 2008).

Involvement of Our Top Differentially Expressed Genes in Astrocyte Function

The top genes that were differentially expressed in our meta-analysis highlight disturbances in a diverse set of astrocytic functions, including the regulation of synaptic transmission.

The downregulation of Sox6 that we observed in our depression models could contribute to the lower astrocyte cell counts and density found in depression. Sox6 is implicated in the differentiation of tissues from all three germ layers during development, including the developing central nervous system and early chondrogenesis in mouse embryos (Ueda et al., 2004). Cell type clusters with the highest expression of Sox6 in the hippocampus include polydendrocytes (oligodendrocyte precursors), ependyma, and astrocytes (Saunders et al., 2018). Sox5/6 double knockouts cause apoptosis and less proliferation of oligodendrocyte precursor cells in the forebrain (Wittstatt et al., 2019). Sox6 also induces astrocyte differentiation. In a study of gene trapping in adult neural stem cells, researchers proved that Sox6 overexpression is sufficient to induce astrocytic differentiation (Scheel et al., 2005). This is consistent with our results indicating downregulation of both Sox6 and other astrocyte-related genes in the animal depression models.

Another gene that we observed to be downregulated in depression models in a manner that could contribute to the decreased astrocytes found in depression is Pamr1, also known as RAMP (regeneration associated muscle protease). Pamr1 has high expression in hippocampal

astrocytes and ependyma cells (Saunders et al., 2018), and functions primarily by binding to calcium ions and breaking serine-type peptide bonds (Safran et al., 2021). Additionally, Pamr1 encodes extracellular matrix molecules (Molofsky, 2014) and is involved in cell proliferation, migration, and phagocytosis (Jeon et al., 2010; Zhou et al., 2015). It may also be involved in the differentiation of neural stem cells into astrocytes, oligodendrocytes, and neurons (Zhou, 2015).

Several of our other top differentially expressed genes are astrocyte-expressed genes that regulate microglial function and neuroimmune processes. The genes Mfge8 (milk fat globule-EGF factor 8) and C3 are highly expressed in the hippocampal astrocyte cell type cluster (Saunders et al., 2018). Mfge8 encodes a preproprotein, which indicates that it can be manipulated post-translation into multiple proteins. Expression of this gene most commonly generates the membrane glycoprotein lactadherin, which contributes to the phagocytic clearance of apoptotic cells (Safran et al., 2021). Specifically, upregulation of Mfge8 leads to microglia-mediated phagocytosis (Spittau et al., 2015). Mfge8 also exhibits phosphatidylethanolamine and phosphatidylserine binding activity (Safran et al., 2021). Among related pathways is the glucocorticoid receptor pathway (Safran et al., 2021), which is integral to the stress response and a target for the GRov and CORT depression models. This gene is also an anti-inflammatory factor (Albus et al., 2016), which is consistent with the observations of neuroinflammation in depression, which would be promoted by the downregulation of Mfge8 shown by our meta-analysis.

The C3 gene activates the complement signaling pathway that controls neuroimmune processes of inflammation and synaptic pruning (Stevens & Johnson, 2021). In addition to astrocyte expression, C3 is most highly expressed in the hippocampal ependyma cell type clusters as well (Saunders et al., 2018). In the brain, astrocytic secretion of C3 binds to C3a receptors on microglia to mediate pathology and neuroinflammation (Lian et al., 2016). This is consistent with our meta-analysis results showing upregulation of C3 in the depression models. Another study linking C3 to astrocyte-microglia communication via the C3-C3aR pathway demonstrated that C3 knockout mice had significantly less microglia-astrocyte interaction (Y. Wei et al., 2021). In the prefrontal cortex, altered C3 expression has shown dramatic effects in mouse models of depression: deletion of C3 is sufficient to rescue synapse loss (Hong et al., 2016) and overexpression of C3 is sufficient to induce depressive-like behavior (Crider et al.,

2018). According to our data, it may be possible that a similar mechanism occurs in the hippocampus, given that C3 was one of the few upregulated genes in our meta-analysis output.

Several of our top differentially expressed genes were implicated in astrocytic regulation of synaptic function, including monoamine oxidase B, or Maob. This gene encodes for an enzyme that catalyzes oxidation-reduction reactions to metabolize monoamines, which generates oxidative stress (Smith et al., 2020). Moab also negatively regulates serotonin secretion and positively regulates dopamine metabolism (Smith et al., 2020). Maob participates in the citalopram pharmacodynamics and pharmacokinetics pathway (Smith et al., 2020), and is clinically targeted for treating psychiatric disorders (Finberg & Rabey, 2016). MAOB polymorphisms compromise mood improvements associated with daily supplementation of tryptophan, the precursor for serotonin (Gonzalez et al., 2021). By inference from the expression pattern in other tissues, Maob is evidenced to respond to corticosterone in rats (Lindley et al., 2005). In the hippocampus, Moab is most highly expressed in astrocyte and ependymal cell-type clusters (Saunders et al., 2018). Astrocytes, similar to neurons, synthesize and release GABA, but use different enzymes. Maob is a key enzyme involved in the synthesis of astrocytic GABA in reactive astrocytes in the hippocampus (Woo et al., 2018, p. 20). Tonic release of GABA leads to extra-synaptic inhibition, also known as tonic current (Bryson et al., 2020; Yoon et al., 2014). Maob knockouts have been shown to eliminate tonic GABA currents in other brain regions, implicating Maob in mediating the balance of neural excitation and inhibition in the brain (Yoon et al., 2014).

This is consistent with other DEGs from our results that are expressed most highly in hippocampal astrocytes and are functionally related to glutamate signaling, including Slc1a3 and Grm3, both downregulated in the hippocampus. Slc1a3 (Solute Carrier Family 1 Member 3) encodes for glutamate-aspartate transporter 1, also known as excitatory amino acid transporter 1 (EAAT1), which transports amino acids and ions across the plasma membrane and mitochondrial membrane (The UniProt Consortium, 2021). This functionality plays a part in the rapid removal of glutamate from the synaptic cleft following an action potential, allowing for the termination of glutamate signaling to the post-synaptic cell ((Ryan et al., 2010), as cited by The UniProt Consortium, 2021)). The downregulation of Slc1a3 in our depression models parallels previous observations from human MDD patients (Medina et al., 2016).

Grm3, also known as GLUR3, is G-protein coupled astrocytic metabotropic glutamate receptor involved in postsynaptic modulation of chemical synaptic transmission. The limited literature on this gene seems split on its involvement in mood disorders such as depression, bipolar disorder, and schizophrenia (Blacker et al., 2017; Dalvie et al., 2010; Jia et al., 2014), with some suggestions of Grm3 as a potential drug target (Blacker et al., 2017). However, another study provides striking evidence of Grm3 contribution to the pathophysiology of MDD: gene expression profiling of micro-dissected postmortem hippocampus of MDD patients showed significant downregulation of GLUR3 (Duric et al., 2013). This is consistent with our meta-analysis results.

In addition to the downregulation of Slc1a3 in our depression models, we also identified additional DEGs encoding solute carriers highly expressed in astrocytes that paralleled observations from human MDD patients (Medina et al., 2016). This may implicate additional facets of homeostatic maintenance through the transport of other macromolecules across the blood-brain barrier, such as Slc27a1 (fatty acid transport) and Slc15a2 (dipeptide transport) (Smith et al., 2020). Notably, downregulation of a fatty acid transporter brings up the discussion of polyunsaturated fatty acid (PUFA) deficiency, which has been previously associated with depression due to its role in healthy neurodevelopment (Hashimoto, 2019; Liao et al., 2019; Müller et al., 2015). Due to high expression of these genes in hippocampal astrocytes, this suggests that astrocytic fatty acid transport may be involved in depression (Moullé et al., 2012). Moreover, PUFA deficiency has been shown to hinder blood-brain barrier function, specifically transport of hydrophilic molecules without a carrier, including amino acid and glucose transport to the brain (Ziylan et al., 1992). Specifically, preclinical findings implicate membrane-forming n-3 PUFAs in the etiology of depression, and this is supported by clinical evidence as well (Müller et al., 2015). Thus, the fatty acid transport of Slc27a1, along with the dipeptide transport of Slc15a2, relates to the findings implicating impaired syncytial functions of astrocytes (Medina et al., 2016).

Comparison of Our Results with Previous Meta-analyses of Depression Models

Our meta-analysis results show some similarities and differences with previous meta-analyses examining hippocampal differential expression in depression models. A recent meta-analysis by Stankiewicz et al. combined 79 animal model studies of stress and 3 human studies

of post-traumatic stress disorder (Stankiewicz et al., 2022). Despite the scale of the study, our results only overlapped with one gene: Fcrls, which was one of the top most frequently and consistently reported genes in two categories of studies defined within Stankiewicz et al: the “all animal data” category, and the "prolonged stress category”. This minimal overlap could be attributed to the inclusion of other types of animal models of depression in our meta-analysis, including genetic susceptibility and altered stress physiology, or the use of human post-traumatic stress disorder results in the Stankiewicz analysis. Moreover, the meta-analysis technique used by Stankiewicz et al. only quantified overlap amongst the top differentially expressed genes identified in individual studies, which predominantly captures genes with extreme effects. These overlapping top genes could be a result of similar confounding variables across multiple studies, which can artificially create overlap. In contrast, our approach of a formal meta-analysis combines effect sizes across studies and thereby minimizes most sources of noise. Formal meta-analyses of effect sizes also often reveal differentially expressed genes that were not significant after FDR correction in the individual studies, but that show consistent direction of effects across studies. Our forest plots (**Figures 2A** and **2B**) illustrate this advantage.

Similarly, another meta-analysis of hippocampal transcriptional profiling studies, Gui et al. 2021, analyzed the overlap between the top genes and pathways from studies of three animal stress models (chronic social defeat stress, chronic unpredictable mild stress, learned helplessness) and human MDD patients (Gui et al., 2021). The results highlighted axon guidance and oligodendrocytes as common functions of their top genes (Gui et al., 2021). Despite similarities to our study, our results did not have any DEGs in common with the top DEGs shared by stress models and MDD patients from Gui et al. The fGSEA analysis run in Gui et al. set a significantly lower permutation test parameter of 1,000 and FDR<0.25, while we used more stringent measures, namely 50,000 permutations and FDR<0.10, increasing the reliability of our findings.

In comparing our results to a meta-analysis of PFC samples from the CSDS model, the similarities are minimal (Reshetnikov et al., 2022). The comparison of DEG lists from the meta-analysis of studies using 10- and 30 day social defeat stress indicates completely distinct results from each other and our own output (Reshetnikov et al., 2022). Yet, similar functional and cell-type expression patterns were enriched within their gene sets as compared to our results. Within the 10-day CSDS analysis, Reshetnikov et al. reports significant enrichment in glucocorticoid

signaling, neuroinflammation, and oxidative stress pathways. Using fGSEA to analyze our meta-analysis output, we found both former pathways enriched, but not the latter. Regarding expression of DEGs in particular cell-types, Reshetnikov et al. saw enrichment with endothelium-specific genes, whereas both fGSEA of our meta-analysis output and cell-type analysis of our top DE genes showed weak, if any, association with of endothelium-specific genes or gene sets. Finally, Reshetnikov et al. found downregulation of a reactive astrocyte-marker (nestin (*Nes*)) (Reshetnikov et al., 2022). This points to the same overarching conclusion of this study: the dysregulation of astrocytic homeostatic function in animal models of depression.

Limitations and Future Directions

This study represents the first formal meta-analysis combining data from diverse animal models and observing their commonalities in the pathology of depression. Yet, it presents many limitations that could be addressed by future studies. First, while we integrated results across multiple distinct models, the HDRF models fall into two groups—genetic susceptibility and stress-related models of depression. Future meta-analysis studies should include models based on other mechanisms for generating depressive-like behavior in animals, such as models of inflammation and insulin resistance. Second, cross-referencing our results with the DropViz database to identify cell-type clusters with the highest hippocampal expression of the top DEGs was implemented for the purpose of identifying possible cell types that were affected in the depression models. Even with limited confirmation by fGSEA, this approach lacked specificity and confidence. A more powerful method to identify cell-type related effects would be to run single-cell RNA-Seq in our samples. Third, depression is an illness with widespread effects in many regions of the brain and is not restricted to the hippocampus. Other important regions include the prefrontal cortex and amygdala, with a significant literature documenting their involvement in depression. Our focus on the hippocampus potentially narrowed our view from a more holistic manifestation of depression in the brain as a circuit-level disorder. Fourth, depression shows considerable sexually dimorphic characteristics in humans and animal models (Labonté et al., 2017). These differences limit the applicability of our findings to females, excluded from our analysis. Further studies are needed to increase the number of female samples

available in the HDRF Data Center to address sex-specific differences and commonalities in the presentation of mood disorder in males and females. Finally, a major question left unanswered by our study revolves around the cause vs. consequence debate – from our results, it is impossible to know whether the gene expression differences found in the hippocampus in our depression models are causal. Further mechanistic studies are necessary to establish causality, through animal studies of gene knockouts and/or targeted cell-type ablations.

Conclusion and Application

In conclusion, within the Hope for Depression Research Foundation, we believe that no single animal model of depression encompasses all aspects of Major Depressive Disorder. Therefore, identifying convergence across models of depression may provide stronger insight into the neurobiology underlying the symptoms and etiology of the disorder. Our meta-analysis results illustrate the power of integrating transcriptional profiling results across different animal models of depression. The findings of this meta-analysis suggest the importance of focusing on glial as well as neuronal mechanisms in seeking to uncover the neurobiological mechanisms of depression. This and similar studies reveal the potential for additional diagnostic indicators and targets of treatment. Previous findings about the role of astrocytes, in particular, indicate that astrocytes not only support neuronal functions through homeostatic regulation, but also influence synaptogenesis, mediate the excitation and inhibition balance, and set the stage for overall neural circuitry (Molofsky, 2014). Therefore, improving the current scientific understanding of how astrocytes, oligodendrocytes, neuroimmune responses, and neurodevelopment work in concert to contribute to depressive symptoms provides expansive opportunities for future research.

References

Akil, H., Gordon, J., Hen, R., Javitch, J., Mayberg, H., McEwen, B., Meaney, M. J., & Nestler, E. J. (2018). Treatment Resistant Depression: A Multi-Scale, Systems Biology Approach. *Neuroscience and Biobehavioral Reviews*, *84*, 272–288. https://doi.org/10.1016/j.neubiorev.2017.08.019

Albus, E., Sinningen, K., Winzer, M., Thiele, S., Baschant, U., Hannemann, A., Fantana, J., Tausche, A.-K., Wallaschofski, H., Nauck, M., Völzke, H., Grossklaus, S., Chavakis, T., Udey, M. C., Hofbauer, L. C., & Rauner, M. (2016). Milk Fat Globule-Epidermal Growth Factor 8 (MFG-E8) Is a Novel Anti-inflammatory Factor in Rheumatoid Arthritis in Mice and Humans. *Journal of Bone and Mineral Research : The Official Journal of the American Society for Bone and Mineral Research*, *31*(3), 596–605. https://doi.org/10.1002/jbmr.2721

Anacker, C., Zunszain, P. A., Carvalho, L. A., & Pariante, C. M. (2011). The glucocorticoid receptor: Pivot of depression and of antidepressant treatment? *Psychoneuroendocrinology*, *36*(3), 415–425. https://doi.org/10.1016/j.psyneuen.2010.03.007

Ardayfio, P., & Kim, K.-S. (20060522). Anxiogenic-like effect of chronic corticosterone in the light-dark emergence task in mice. *Behavioral Neuroscience*, *120*(2), 249. https://doi.org/10.1037/0735-7044.120.2.249

Bachmann, S. (2018). Epidemiology of Suicide and the Psychiatric Perspective. *International Journal of Environmental Research and Public Health*, *15*(7), 1425. https://doi.org/10.3390/ijerph15071425

Badr, A. M., Attia, H. A., & Al-Rasheed, N. (2020). Oleuropein Reverses Repeated Corticosterone-Induced Depressive-Like Behavior in mice: Evidence of Modulating

Effect on Biogenic Amines. *Scientific Reports*, *10*(1), Article 1. https://doi.org/10.1038/s41598-020-60026-1

Bagot, R. C., Cates, H. M., Purushothaman, I., Lorsch, Z. S., Walker, D. M., Wang, J., Huang, X., Schlüter, O. M., Maze, I., Peña, C. J., Heller, E. A., Issler, O., Wang, M., Song, W., Stein, J. L., Liu, X., Doyle, M. A., Scobie, K. N., Sun, H. S., … Nestler, E. J. (2016). Circuit-wide Transcriptional Profiling Reveals Brain Region-Specific Gene Networks Regulating Depression Susceptibility. *Neuron*, *90*(5), 969–983. https://doi.org/10.1016/j.neuron.2016.04.015

Bagot, R. C., Cates, H. M., Purushothaman, I., Vialou, V., Heller, E. A., Yieh, L., LaBonté, B., Peña, C. J., Shen, L., Wittenberg, G. M., & Nestler, E. J. (2017). Ketamine and Imipramine Reverse Transcriptional Signatures of Susceptibility and Induce Resilience-Specific Gene Expression Profiles. *Biological Psychiatry*, *81*(4), 285–295. https://doi.org/10.1016/j.biopsych.2016.06.012

Banasr, M., & Duman, R. S. (2008). Glial loss in the prefrontal cortex is sufficient to induce depressive-like behaviors. *Biological Psychiatry*, *64*(10), 863–870. https://doi.org/10.1016/j.biopsych.2008.06.008

Belleau, E. L., Treadway, M. T., & Pizzagalli, D. A. (2019). The Impact of Stress and Major Depressive Disorder on Hippocampal and Medial Prefrontal Cortex Morphology. *Biological Psychiatry*, *85*(6), 443–453. https://doi.org/10.1016/j.biopsych.2018.09.031

Belzung, C., & Lemoine, M. (2011). Criteria of validity for animal models of psychiatric disorders: Focus on anxiety disorders and depression. *Biology of Mood & Anxiety Disorders*, *1*(1), 9. https://doi.org/10.1186/2045-5380-1-9

Berger, S., Gureczny, S., Reisinger, S. N., Horvath, O., & Pollak, D. D. (2019). Effect of Chronic Corticosterone Treatment on Depression-Like Behavior and Sociability in Female and Male C57BL/6N Mice. *Cells*, *8*(9), 1018. https://doi.org/10.3390/cells8091018

Birt, I. A., Hagenauer, M. H., Clinton, S. M., Aydin, C., Blandino, P., Stead, J. D. H., Hilde, K. L., Meng, F., Thompson, R. C., Khalil, H., Stefanov, A., Maras, P., Zhou, Z., Hebda-Bauer, E. K., Goldman, D., Watson, S. J., & Akil, H. (2021). Genetic Liability for Internalizing Versus Externalizing Behavior Manifests in the Developing and Adult Hippocampus: Insight From a Meta-analysis of Transcriptional Profiling Studies in a Selectively Bred Rat Model. *Biological Psychiatry*, *89*(4), 339–355. https://doi.org/10.1016/j.biopsych.2020.05.024

Blacker, C. J., Lewis, C. P., Frye, M. A., & Veldic, M. (2017). Metabotropic glutamate receptors as emerging research targets in bipolar disorder. *Psychiatry Research*, *257*, 327–337. https://doi.org/10.1016/j.psychres.2017.07.059

Blaveri, E., Kelly, F., Mallei, A., Harris, K., Taylor, A., Reid, J., Razzoli, M., Carboni, L., Piubelli, C., Musazzi, L., Racagni, G., Mathé, A., Popoli, M., Domenici, E., & Bates, S. (2010). Expression Profiling of a Genetic Animal Model of Depression Reveals Novel Molecular Pathways Underlying Depressive-Like Behaviours. *PLoS ONE*, *5*(9), e12596. https://doi.org/10.1371/journal.pone.0012596

Bogdanova, O. V., Kanekar, S., D'Anci, K. E., & Renshaw, P. F. (2013). Factors influencing behavior in the forced swim test. *Physiology & Behavior*, *118*, 227–239. https://doi.org/10.1016/j.physbeh.2013.05.012

Bryson, A., Hatch, R. J., Zandt, B.-J., Rossert, C., Berkovic, S. F., Reid, C. A., Grayden, D. B., Hill, S. L., & Petrou, S. (2020). GABA-mediated tonic inhibition differentially modulates gain in functional subtypes of cortical interneurons. *Proceedings of the National Academy of Sciences*, *117*(6), 3192–3202. https://doi.org/10.1073/pnas.1906369117

Button, K. S., Ioannidis, J. P. A., Mokrysz, C., Nosek, B. A., Flint, J., Robinson, E. S. J., & Munafò, M. R. (2013). Power failure: Why small sample size undermines the reliability of neuroscience. *Nature Reviews Neuroscience*, *14*(5), Article 5. https://doi.org/10.1038/nrn3475

Caffrey, M. (2017). *With Anxiety Common in Depression, DSM-5 Specifier Aids Screening*. AJMC. https://www.ajmc.com/view/with-anxiety-common-in-depression-dsm-5-specifier-aids-screening

Can, A., Dao, D. T., Terrillion, C. E., Piantadosi, S. C., Bhat, S., & Gould, T. D. (2012). The Tail Suspension Test. *Journal of Visualized Experiments : JoVE*, *59*, 3769. https://doi.org/10.3791/3769

Caradonna, S. G., Zhang, T.-Y., O'Toole, N., Shen, M.-J., Khalil, H., Einhorn, N. R., Wen, X., Parent, C., Lee, F. S., Akil, H., Meaney, M. J., McEwen, B. S., & Marrocco, J. (2022). Genomic modules and intramodular network concordance in susceptible and resilient male mice across models of stress. *Neuropsychopharmacology: Official Publication of the American College of Neuropsychopharmacology*, *47*(5), 987–999. https://doi.org/10.1038/s41386-021-01219-8

Chan, J. N.-M., Lee, J. C.-D., Lee, S. S. P., Hui, K. K. Y., Chan, A. H. L., Fung, T. K.-H., Sánchez-Vidaña, D. I., Lau, B. W.-M., & Ngai, S. P.-C. (2017). Interaction Effect of Social Isolation and High Dose Corticosteroid on Neurogenesis and Emotional Behavior.

Frontiers in Behavioral Neuroscience, *11*. https://www.frontiersin.org/article/10.3389/fnbeh.2017.00018

Chow, W., Doane, M. J., Sheehan, J., Alphs, L., & Le, H. (n.d.). *Economic Burden Among Patients With Major Depressive Disorder: An Analysis of Healthcare Resource Use, Work Productivity, and Direct and Indirect Costs by Depression Severity*. AJMC. Retrieved August 25, 2021, from https://www.ajmc.com/view/economic-burden-mdd

Cooper, J. A., Arulpragasam, A. R., & Treadway, M. T. (2018). Anhedonia in depression: Biological mechanisms and computational models. *Current Opinion in Behavioral Sciences*, *22*, 128–135. https://doi.org/10.1016/j.cobeha.2018.01.024

Crider, A., Feng, T., Pandya, C. D., Davis, T., Nair, A., Ahmed, A. O., Baban, B., Turecki, G., & Pillai, A. (2018). Complement component 3a receptor deficiency attenuates chronic stress-induced monocyte infiltration and depressive-like behavior. *Brain, Behavior, and Immunity*, *70*, 246–256. https://doi.org/10.1016/j.bbi.2018.03.004

Dai, M., Wang, P., Boyd, A. D., Kostov, G., Athey, B., Jones, E. G., Bunney, W. E., Myers, R. M., Speed, T. P., Akil, H., Watson, S. J., & Meng, F. (2005). Evolving gene/transcript definitions significantly alter the interpretation of GeneChip data. *Nucleic Acids Research*, *33*(20), e175. https://doi.org/10.1093/nar/gni179

Dalvie, S., Horn, N., Nossek, C., van der Merwe, L., Stein, D. J., & Ramesar, R. (2010). Psychosis and relapse in bipolar disorder are related to GRM3, DAOA, and GRIN2B genotype. *African Journal of Psychiatry*, *13*(4), 297–301. https://doi.org/10.4314/ajpsy.v13i4.61880

David, D. J., Samuels, B. A., Rainer, Q., Wang, J.-W., Marsteller, D., Mendez, I., Drew, M., Craig, D. A., Guiard, B. P., Guilloux, J.-P., Artymyshyn, R. P., Gardier, A. M., Gerald,

C., Antonijevic, I. A., Leonardo, E. D., & Hen, R. (2009). Neurogenesis-Dependent and -Independent Effects of Fluoxetine in an Animal Model of Anxiety/Depression. *Neuron*, *62*(4), 479–493. https://doi.org/10.1016/j.neuron.2009.04.017

Detke, M. J., Rickels, M., & Lucki, I. (1995). Active behaviors in the rat forced swimming test differentially produced by serotonergic and noradrenergic antidepressants. *Psychopharmacology*, *121*(1), 66–72. https://doi.org/10.1007/BF02245592

Diagnostic and Statistical Manual of Mental Disorders. (2013). https://dsm-psychiatryonline-org.proxy.lib.umich.edu/doi/epdf/10.1176/appi.books.9780890425596

Dieterich, A., Srivastava, P., Sharif, A., Stech, K., Floeder, J., Yohn, S. E., & Samuels, B. A. (2019). Chronic corticosterone administration induces negative valence and impairs positive valence behaviors in mice. *Translational Psychiatry*, *9*(1), Article 1. https://doi.org/10.1038/s41398-019-0674-4

Dranovsky, A., & Hen, R. (2006). Hippocampal Neurogenesis: Regulation by Stress and Antidepressants. *Biological Psychiatry*, *59*(12), 1136–1143. https://doi.org/10.1016/j.biopsych.2006.03.082

Duman, C. H. (2010). Models of Depression. In *Vitamins & Hormones* (Vol. 82, pp. 1–21). Elsevier. https://doi.org/10.1016/S0083-6729(10)82001-1

Duric, V., Banasr, M., Stockmeier, C. A., Simen, A. A., Newton, S. S., Overholser, J. C., Jurjus, G. J., Dieter, L., & Duman, R. S. (2013). Altered expression of synapse and glutamate related genes in post-mortem hippocampus of depressed subjects. *The International Journal of Neuropsychopharmacology / Official Scientific Journal of the Collegium Internationale Neuropsychopharmacologicum (CINP)*, *16*(1), 69–82. https://doi.org/10.1017/S1461145712000016

Estanislau, C., Ramos, A. C., Ferraresi, P. D., Costa, N. F., de Carvalho, H. M. C. P., & Batistela, S. (2011). Individual differences in the elevated plus-maze and the forced swim test. *Behavioural Processes*, *86*(1), 46–51. https://doi.org/10.1016/j.beproc.2010.08.008

Fava, M., Alpert, J. E., Carmin, C. N., Wisniewski, S. R., Trivedi, M. H., Biggs, M. M., Shores-Wilson, K., Morgan, D., Schwartz, T., Balasubramani, G. K., & Rush, A. J. (2004). Clinical correlates and symptom patterns of anxious depression among patients with major depressive disorder in STAR*D. *Psychological Medicine*, *34*(7), 1299–1308. https://doi.org/10.1017/s0033291704002612

Fava, M., Rush, A. J., Alpert, J. E., Balasubramani, G. K., Wisniewski, S. R., Carmin, C. N., Biggs, M. M., Zisook, S., Leuchter, A., Howland, R., Warden, D., & Trivedi, M. H. (2008). Difference in treatment outcome in outpatients with anxious versus nonanxious depression: A STAR*D report. *The American Journal of Psychiatry*, *165*(3), 342–351. https://doi.org/10.1176/appi.ajp.2007.06111868

Ferreira-Nuño, A., Overstreet, D. H., Morales-Otal, A., & Velázquez-Moctezuma, J. (2002). Masculine sexual behavior features in the Flinders sensitive and resistant line rats. *Behavioural Brain Research*, *128*(2), 113–119. https://doi.org/10.1016/S0166-4328(01)00313-8

Finberg, J. P. M., & Rabey, J. M. (2016). Inhibitors of MAO-A and MAO-B in Psychiatry and Neurology. *Frontiers in Pharmacology*, *7*, 340. https://doi.org/10.3389/fphar.2016.00340

Flagel, S. B., Waselus, M., Clinton, S. M., Watson, S. J., & Akil, H. (2014). Antecedents and consequences of drug abuse in rats selectively bred for high and low response to novelty. *Neuropharmacology*, *76 Pt B*, 425–436. https://doi.org/10.1016/j.neuropharm.2013.04.033

Flint, J., & Kendler, K. S. (2014). The Genetics of Major Depression. *Neuron*, *81*(3), 484–503. https://doi.org/10.1016/j.neuron.2014.01.027

Fuchs, E., & Flügge, G. (2006). Experimental animal models for the simulation of depression and anxiety. *Dialogues in Clinical Neuroscience*, *8*(3), 323–333.

Golden, S. A., Covington, H. E., Berton, O., & Russo, S. J. (2011). A standardized protocol for repeated social defeat stress in mice. *Nature Protocols*, *6*(8), 1183–1191. https://doi.org/10.1038/nprot.2011.361

Gonzalez, I., Polvillo, R., Ruiz-Galdon, M., Reyes-Engel, A., & Royo, J. L. (2021). MAOB rs3027452 Modifies Mood Improvement After Tryptophan Supplementation. *International Journal of General Medicine*, *14*, 1751–1756. https://doi.org/10.2147/IJGM.S305443

Gray, R. S., Wilm, T. P., Smith, J., Bagnat, M., Dale, R. M., Topczewski, J., Johnson, S. L., & Solnica-Krezel, L. (2014). Loss of col8a1a function during zebrafish embryogenesis results in congenital vertebral malformations. *Developmental Biology*, *386*(1), 72–85. https://doi.org/10.1016/j.ydbio.2013.11.028

Greenberg, P. E., Fournier, A.-A., Sisitsky, T., Simes, M., Berman, R., Koenigsberg, S. H., & Kessler, R. C. (2021). The Economic Burden of Adults with Major Depressive Disorder in the United States (2010 and 2018). *PharmacoEconomics*, *39*(6), 653–665. https://doi.org/10.1007/s40273-021-01019-4

Groen, R. N., Ryan, O., Wigman, J. T. W., Riese, H., Penninx, B. W. J. H., Giltay, E. J., Wichers, M., & Hartman, C. A. (2020). Comorbidity between depression and anxiety: Assessing the role of bridge mental states in dynamic psychological networks. *BMC Medicine*, *18*, 308. https://doi.org/10.1186/s12916-020-01738-z

Gui, S., Liu, Y., Pu, J., Song, X., Chen, X., Chen, W., Zhong, X., Wang, H., Liu, L., & Xie, P. (2021). Comparative analysis of hippocampal transcriptional features between major depressive disorder patients and animal models. *Journal of Affective Disorders*, *293*, 19–28. https://doi.org/10.1016/j.jad.2021.06.007

Hagenauer, M. H., Schulmann, A., Li, J. Z., Vawter, M. P., Walsh, D. M., Thompson, R. C., Turner, C. A., Bunney, W. E., Myers, R. M., Barchas, J. D., Schatzberg, A. F., Watson, S. J., & Akil, H. (2018). Inference of cell type content from human brain transcriptomic datasets illuminates the effects of age, manner of death, dissection, and psychiatric diagnosis. *PloS One*, *13*(7), e0200003. https://doi.org/10.1371/journal.pone.0200003

Hammels, C., Pishva, E., De Vry, J., van den Hove, D. L. A., Prickaerts, J., van Winkel, R., Selten, J.-P., Lesch, K.-P., Daskalakis, N. P., Steinbusch, H. W. M., van Os, J., Kenis, G., & Rutten, B. P. F. (2015). Defeat stress in rodents: From behavior to molecules. *Neuroscience and Biobehavioral Reviews*, *59*, 111–140. https://doi.org/10.1016/j.neubiorev.2015.10.006

Hashimoto, K. (2019). Role of Soluble Epoxide Hydrolase in Metabolism of PUFAs in Psychiatric and Neurological Disorders. *Frontiers in Pharmacology*, *10*, 36. https://doi.org/10.3389/fphar.2019.00036

HDRF Gene Explorer. (2022, August 29). https://hdrf-dtf.org/login/genex/

Hebda-Bauer, E. K., Pletsch, A., Darwish, H., Fentress, H., Simmons, T. A., Wei, Q., Watson, S. J., & Akil, H. (2010). Forebrain Glucocorticoid Receptor Overexpression Increases Environmental Reactivity and Produces a Stress-Induced Spatial Discrimination Deficit. *Neuroscience*, *169*(2), 645–653. https://doi.org/10.1016/j.neuroscience.2010.05.033

Hettema, J. M. (2008). What is the genetic relationship between anxiety and depression? *American Journal of Medical Genetics Part C: Seminars in Medical Genetics*, *148C*(2), 140–146. https://doi.org/10.1002/ajmg.c.30171

Hong, S., Beja-Glasser, V. F., Nfonoyim, B. M., Frouin, A., Li, S., Ramakrishnan, S., Merry, K. M., Shi, Q., Rosenthal, A., Barres, B. A., Lemere, C. A., Selkoe, D. J., & Stevens, B. (2016). Complement and microglia mediate early synapse loss in Alzheimer mouse models. *Science*, *352*(6286), 712–716. https://doi.org/10.1126/science.aad8373

Hu, J., Bibli, S.-I., Wittig, J., Zukunft, S., Lin, J., Hammes, H.-P., Popp, R., & Fleming, I. (2019). Soluble epoxide hydrolase promotes astrocyte survival in retinopathy of prematurity. *The Journal of Clinical Investigation*, *129*(12), 5204–5218. https://doi.org/10.1172/JCI123835

James, S. L., Abate, D., Abate, K. H., Abay, S. M., Abbafati, C., Abbasi, N., Abbastabar, H., Abd-Allah, F., Abdela, J., Abdelalim, A., Abdollahpour, I., Abdulkader, R. S., Abebe, Z., Abera, S. F., Abil, O. Z., Abraha, H. N., Abu-Raddad, L. J., Abu-Rmeileh, N. M. E., Accrombessi, M. M. K., … Murray, C. J. L. (2018). Global, regional, and national incidence, prevalence, and years lived with disability for 354 diseases and injuries for 195 countries and territories, 1990–2017: A systematic analysis for the Global Burden of Disease Study 2017. *The Lancet*, *392*(10159), 1789–1858. https://doi.org/10.1016/S0140-6736(18)32279-7

Jeon, H., Go, Y., Seo, M., Lee, W.-H., & Suk, K. (2010). Functional Selection of Phagocytosis-Promoting Genes: Cell Sorting–Based Selection. *Journal of Biomolecular Screening*, *15*(8), 949–955. https://doi.org/10.1177/1087057110376090

Jia, W., Zhang, R., Wu, B., Dai, Z., Zhu, Y., Li, P., & Zhu, F. (2014). Metabotropic glutamate receptor 3 is associated with heroin dependence but not depression or schizophrenia in a Chinese population. *PloS One*, *9*(1), e87247. https://doi.org/10.1371/journal.pone.0087247

Kalin, N. H. (2020). The Critical Relationship Between Anxiety and Depression. *American Journal of Psychiatry*, *177*(5), 365–367. https://doi.org/10.1176/appi.ajp.2020.20030305

Karabeg, M. M., Grauthoff, S., Kollert, S. Y., Weidner, M., Heiming, R. S., Jansen, F., Popp, S., Kaiser, S., Lesch, K.-P., Sachser, N., Schmitt, A. G., & Lewejohann, L. (2013). 5-HTT Deficiency Affects Neuroplasticity and Increases Stress Sensitivity Resulting in Altered Spatial Learning Performance in the Morris Water Maze but Not in the Barnes Maze. *PLOS ONE*, *8*(10), e78238. https://doi.org/10.1371/journal.pone.0078238

Keitner, G. I., & Miller, I. W. (1990). Family functioning and major depression: An overview. *The American Journal of Psychiatry*, *147*(9), 1128–1137. https://doi.org/10.1176/ajp.147.9.1128

Kerman, I. A., Clinton, S. M., Bedrosian, T. A., Abraham, A. D., Rosenthal, D. T., Akil, H., & Watson, S. J. (2011). High novelty-seeking predicts aggression and gene expression differences within defined serotonergic cell groups. *Brain Research*, *1419*, 34–45. https://doi.org/10.1016/j.brainres.2011.08.038

Kessler, R. C., Sampson, N. A., Berglund, P., Gruber, M. J., Al-Hamzawi, A., Andrade, L., Bunting, B., Demyttenaere, K., Florescu, S., de Girolamo, G., Gureje, O., He, Y., Hu, C., Huang, Y., Karam, E., Kovess-Masfety, V., Lee, S., Levinson, D., Medina Mora, M. E., … Wilcox, M. A. (2015). Anxious and non-anxious major depressive disorder in the

World Health Organization World Mental Health Surveys. *Epidemiology and Psychiatric Sciences*, *24*(3), 210–226. https://doi.org/10.1017/S2045796015000189

Kessler, R. C., & Wang, P. S. (2008). The descriptive epidemiology of commonly occurring mental disorders in the United States. *Annual Review of Public Health*, *29*, 115–129. https://doi.org/10.1146/annurev.publhealth.29.020907.090847

Kinsey, S. G., Bailey, M. T., Sheridan, J. F., Padgett, D. A., & Avitsur, R. (2007). Repeated social defeat causes increased anxiety-like behavior and alters splenocyte function in C57BL/6 and CD-1 mice. *Brain, Behavior, and Immunity*, *21*(4), 458–466. https://doi.org/10.1016/j.bbi.2006.11.001

Kolber, B. J., Wieczorek, L., & Muglia, L. J. (2008). HPA axis dysregulation and behavioral analysis of mouse mutants with altered GR or MR function. *Stress (Amsterdam, Netherlands)*, *11*(5), 321–338. https://doi.org/10.1080/10253890701821081

Kollack-Walker, S., Watson, S. J., & Akil, H. (1997). Social Stress in Hamsters: Defeat Activates Specific Neurocircuits within the Brain. *The Journal of Neuroscience*, *17*(22), 8842–8855. https://doi.org/10.1523/JNEUROSCI.17-22-08842.1997

Komada, M., Takao, K., & Miyakawa, T. (2008). Elevated Plus Maze for Mice. *Journal of Visualized Experiments : JoVE*, *22*, 1088. https://doi.org/10.3791/1088

Koonin, E. V. (2005). Orthologs, Paralogs, and Evolutionary Genomics. *Annual Review of Genetics*, *39*(1), 309–338. https://doi.org/10.1146/annurev.genet.39.073003.114725

Krishnan, V., Han, M.-H., Graham, D. L., Berton, O., Renthal, W., Russo, S. J., LaPlant, Q., Graham, A., Lutter, M., Lagace, D. C., Ghose, S., Reister, R., Tannous, P., Green, T. A., Neve, R. L., Chakravarty, S., Kumar, A., Eisch, A. J., Self, D. W., … Nestler, E. J. (2007). Molecular Adaptations Underlying Susceptibility and Resistance to Social Defeat

in Brain Reward Regions. *Cell*, *131*(2), 391–404. https://doi.org/10.1016/j.cell.2007.09.018

Krishnan, V., & Nestler, E. J. (2011a). Animal Models of Depression: Molecular Perspectives. *Current Topics in Behavioral Neurosciences*, *7*, 121–147. https://doi.org/10.1007/7854_2010_108

Krishnan, V., & Nestler, E. J. (2011b). Animal Models of Depression: Molecular Perspectives. *Current Topics in Behavioral Neurosciences*, *7*, 121–147. https://doi.org/10.1007/7854_2010_108

Kukurba, K. R., & Montgomery, S. B. (2015). RNA Sequencing and Analysis. *Cold Spring Harbor Protocols*, *2015*(11), 951–969. https://doi.org/10.1101/pdb.top084970

Labonté, B., Engmann, O., Purushothaman, I., Menard, C., Wang, J., Tan, C., Scarpa, J. R., Moy, G., Loh, Y.-H. E., Cahill, M., Lorsch, Z. S., Hamilton, P. J., Calipari, E. S., Hodes, G. E., Issler, O., Kronman, H., Pfau, M., Obradovic, A., Dong, Y., … Nestler, E. J. (2017). Sex-Specific Transcriptional Signatures in Human Depression. *Nature Medicine*, *23*(9), 1102–1111. https://doi.org/10.1038/nm.4386

Lakens, D. (2013). Calculating and reporting effect sizes to facilitate cumulative science: A practical primer for t-tests and ANOVAs. *Frontiers in Psychology*, *4*. https://www.frontiersin.org/articles/10.3389/fpsyg.2013.00863

Lian, H., Litvinchuk, A., Chiang, A. C.-A., Aithmitti, N., Jankowsky, J. L., & Zheng, H. (2016). Astrocyte-Microglia Cross Talk through Complement Activation Modulates Amyloid Pathology in Mouse Models of Alzheimer's Disease. *The Journal of Neuroscience*, *36*(2), 577–589. https://doi.org/10.1523/JNEUROSCI.2117-15.2016

Liao, Y., Xie, B., Zhang, H., He, Q., Guo, L., Subramanieapillai, M., Fan, B., Lu, C., & McIntyre, R. S. (2019). Efficacy of omega-3 PUFAs in depression: A meta-analysis. *Translational Psychiatry*, *9*, 190. https://doi.org/10.1038/s41398-019-0515-5

Lindley, S. E., She, X., & Schatzberg, A. F. (2005). Monoamine oxidase and catechol-o-methyltransferase enzyme activity and gene expression in response to sustained glucocorticoids. *Psychoneuroendocrinology*, *30*(8), 785–790. https://doi.org/10.1016/j.psyneuen.2005.03.007

Liu, M.-Y., Yin, C.-Y., Zhu, L.-J., Zhu, X.-H., Xu, C., Luo, C.-X., Chen, H., Zhu, D.-Y., & Zhou, Q.-G. (2018). Sucrose preference test for measurement of stress-induced anhedonia in mice. *Nature Protocols*, *13*(7), Article 7. https://doi.org/10.1038/s41596-018-0011-z

Malone, J. H., & Oliver, B. (2011). Microarrays, deep sequencing and the true measure of the transcriptome. *BMC Biology*, *9*, 34. https://doi.org/10.1186/1741-7007-9-34

Marrocco, J., Einhorn, N. R., Petty, G. H., Li, H., Dubey, N., Hoffman, J., Berman, K. F., Goldman, D., Lee, F. S., Schmidt, P. J., & McEwen, B. S. (2020). Epigenetic intersection of BDNF Val66Met genotype with premenstrual dysphoric disorder transcriptome in a cross-species model of estradiol add-back. *Molecular Psychiatry*, *25*(3), 572–583. https://doi.org/10.1038/s41380-018-0274-3

McEwen, B. S., & Akil, H. (2020). Revisiting the Stress Concept: Implications for Affective Disorders. *The Journal of Neuroscience*, *40*(1), 12–21. https://doi.org/10.1523/JNEUROSCI.0733-19.2019

McEwen, B. S., Weiss, J. M., & Schwartz, L. S. (1968). Selective retention of corticosterone by limbic structures in rat brain. *Nature*, *220*(5170), 911–912. https://doi.org/10.1038/220911a0

Medina, A., Watson, S. J., Bunney, W., Myers, R. M., Schatzberg, A., Barchas, J., Akil, H., & Thompson, R. C. (2016). Evidence for alterations of the glial syncytial function in major depressive disorder. *Journal of Psychiatric Research*, *72*, 15–21. https://doi.org/10.1016/j.jpsychires.2015.10.010

Melartin, T. K., Rytsälä, H. J., Leskelä, U. S., Lestelä-Mielonen, P. S., Sokero, T. P., & Isometsä, E. T. (2002). Current comorbidity of psychiatric disorders among DSM-IV major depressive disorder patients in psychiatric care in the Vantaa Depression Study. *The Journal of Clinical Psychiatry*, *63*(2), 126–134.

Melas, P. A., Wirf, M., André, H., Jayaram-Lindström, N., Mathé, A. A., & Steensland, P. (2021). The monoamine stabilizer OSU6162 has anxiolytic-like properties and reduces voluntary alcohol intake in a genetic rat model of depression. *Scientific Reports*, *11*(1), Article 1. https://doi.org/10.1038/s41598-021-91215-1

Meshalkina, D. A., & Kalueff, A. V. (2016). Commentary: Ethological Evaluation of the Effects of Social Defeat Stress in Mice: Beyond the Social Interaction Ratio. *Frontiers in Behavioral Neuroscience*, *10*. https://www.frontiersin.org/article/10.3389/fnbeh.2016.00155

Moullé, V. S. F., Cansell, C., Luquet, S., & Cruciani-Guglielmacci, C. (2012). The multiple roles of fatty acid handling proteins in brain. *Frontiers in Physiology*, *3*, 385. https://doi.org/10.3389/fphys.2012.00385

Müller, C. P., Reichel, M., Mühle, C., Rhein, C., Gulbins, E., & Kornhuber, J. (2015). Brain membrane lipids in major depression and anxiety disorders. *Biochimica et Biophysica Acta (BBA) - Molecular and Cell Biology of Lipids*, *1851*(8), 1052–1065. https://doi.org/10.1016/j.bbalip.2014.12.014

Murra, D., Hilde, K. L., Fitzpatrick, A., Maras, P. M., Watson, S. J., & Akil, H. (2022). Characterizing the behavioral and neuroendocrine features of susceptibility and resilience to social stress. *Neurobiology of Stress*, *17*, 100437. https://doi.org/10.1016/j.ynstr.2022.100437

Nestler, E. J., & Hyman, S. E. (2010). Animal Models of Neuropsychiatric Disorders. *Nature Neuroscience*, *13*(10), 1161–1169. https://doi.org/10.1038/nn.2647

O'Donnell, K. J., & Meaney, M. J. (2017). Fetal Origins of Mental Health: The Developmental Origins of Health and Disease Hypothesis. *The American Journal of Psychiatry*, *174*(4), 319–328. https://doi.org/10.1176/appi.ajp.2016.16020138

Overstreet, D. H., & Wegener, G. (2013). The Flinders Sensitive Line Rat Model of Depression—25 Years and Still Producing. *Pharmacological Reviews*, *65*(1), 143–155. https://doi.org/10.1124/pr.111.005397

Pellow, S., Chopin, P., File, S. E., & Briley, M. (1985). Validation of open:closed arm entries in an elevated plus-maze as a measure of anxiety in the rat. *Journal of Neuroscience Methods*, *14*(3), 149–167. https://doi.org/10.1016/0165-0270(85)90031-7

Porsolt, R. D., Le Pichon, M., & Jalfre, M. (1977). Depression: A new animal model sensitive to antidepressant treatments. *Nature*, *266*(5604), 730–732. https://doi.org/10.1038/266730a0

Pucilowski, O., Overstreet, D. H., Rezvani, A. H., & Janowsky, D. S. (1993). Chronic mild stress-induced anhedonia: Greater effect in a genetic rat model of depression. *Physiology & Behavior*, *54*(6), 1215–1220. https://doi.org/10.1016/0031-9384(93)90351-F

Research on Depression. (n.d.). Hope For Depression. Retrieved September 6, 2022, from https://www.hopefordepression.org/research-funding-and-impact/

Reshetnikov, V. V., Kisaretova, P. E., & Bondar, N. P. (2022). Transcriptome Alterations Caused by Social Defeat Stress of Various Durations in Mice and Its Relevance to Depression and Posttraumatic Stress Disorder in Humans: A Meta-Analysis. *International Journal of Molecular Sciences*, *23*(22), 13792. https://doi.org/10.3390/ijms232213792

Ritchie, M. E., Phipson, B., Wu, D., Hu, Y., Law, C. W., Shi, W., & Smyth, G. K. (2015). Limma powers differential expression analyses for RNA-sequencing and microarray studies | Nucleic Acids Research | Oxford Academic. *Nucleic Acids Research*, *43*(7). https://doi.org/10.1093/nar/gkv007

Rush, A. J., Trivedi, M. H., Wisniewski, S. R., Nierenberg, A. A., Stewart, J. W., Warden, D., Niederehe, G., Thase, M. E., Lavori, P. W., Lebowitz, B. D., McGrath, P. J., Rosenbaum, J. F., & Sackeim, H. A. (2006). Acute and Longer-Term Outcomes in Depressed Outpatients Requiring One or Several Treatment Steps: A STAR*D Report. *Am J Psychiatry*, 13.

Ryan, R. M., Kortt, N. C., Sirivanta, T., & Vandenberg, R. J. (2010). The position of an arginine residue influences substrate affinity and K+ coupling in the human glutamate transporter, EAAT1. *Journal of Neurochemistry*, *114*(2), 565–575. https://doi.org/10.1111/j.1471-4159.2010.06796.x

Safran, M., Rosen, N., Twik, M., BarShir, R., Stein, T. I., Dahary, D., Fishilevich, S., & Lancet, D. (2021). The GeneCards Suite. In I. Abugessaisa & T. Kasukawa (Eds.), *Practical Guide to Life Science Databases* (pp. 27–56). Springer Nature. https://doi.org/10.1007/978-981-16-5812-9_2

Samuels, B. A., Leonardo, E. D., Dranovsky, A., Williams, A., Wong, E., Nesbitt, A. M. I., McCurdy, R. D., Hen, R., & Alter, M. (2014). Global state measures of the dentate gyrus gene expression system predict antidepressant-sensitive behaviors. *PloS One*, *9*(1), e85136. https://doi.org/10.1371/journal.pone.0085136

Saunders, A., Macosko, E., Wysoker, A., Goldman, M., Krienen, F., de Rivera, H., Bien, E., Baum, M., Wang, S., Goeva, A., Nemesh, J., Kamitaki, N., Brumbaugh, S., Kulp, D., & McCarroll, S. A. (2018). Molecular Diversity and Specializations among the Cells of the Adult Mouse Brain. *Cell*, *174*(4), 1015-1030.e16. https://doi.org/10.1016/j.cell.2018.07.028

Scheel, J. R., Ray, J., Gage, F. H., & Barlow, C. (2005). Quantitative analysis of gene expression in living adult neural stem cells by gene trapping. *Nature Methods*, *2*(5), 363–370. https://doi.org/10.1038/nmeth755

Sergushichev, A. A. (2016). *An algorithm for fast preranked gene set enrichment analysis using cumulative statistic calculation* (p. 060012). https://doi.org/10.1101/060012

Sheline, Y. I., Wang, P. W., Gado, M. H., Csernansky, J. G., & Vannier, M. W. (1996). Hippocampal atrophy in recurrent major depression. *Proceedings of the National Academy of Sciences of the United States of America*, *93*(9), 3908–3913. https://doi.org/10.1073/pnas.93.9.3908

Smith, J. R., Hayman, G. T., Wang, S.-J., Laulederkind, S. J. F., Hoffman, M. J., Kaldunski, M. L., Tutaj, M., Thota, J., Nalabolu, H. S., Ellanki, S. L. R., Tutaj, M. A., De Pons, J. L., Kwitek, A. E., Dwinell, M. R., & Shimoyama, M. E. (2020). The Year of the Rat: The Rat Genome Database at 20: a multi-species knowledgebase and analysis platform. *Nucleic Acids Research*, *48*(D1), D731–D742. https://doi.org/10.1093/nar/gkz1041

Sobieraj, M., Williams, J., Marley, J., & Ryan, P. (1998). The impact of depression on the physical health of family members. *The British Journal of General Practice*, *48*(435), 1653–1655.

Spittau, B., Rilka, J., Steinfath, E., Zöller, T., & Krieglstein, K. (2015). TGFβ1 increases microglia-mediated engulfment of apoptotic cells via upregulation of the milk fat globule-EGF factor 8. *Glia*, *63*(1), 142–153. https://doi.org/10.1002/glia.22740

Stankiewicz, A. M., Jaszczyk, A., Goscik, J., & Juszczak, G. R. (2022). Stress and the brain transcriptome: Identifying commonalities and clusters in standardized data from published experiments. *Progress in Neuro-Psychopharmacology & Biological Psychiatry*, *119*, 110558. https://doi.org/10.1016/j.pnpbp.2022.110558

Stead, J. D. H., Clinton, S., Neal, C., Schneider, J., Jama, A., Miller, S., Vazquez, D. M., Watson, S. J., & Akil, H. (2006). Selective breeding for divergence in novelty-seeking traits: Heritability and enrichment in spontaneous anxiety-related behaviors. *Behavior Genetics*, *36*(5), 697–712. https://doi.org/10.1007/s10519-006-9058-7

Stedenfeld, K. A., Clinton, S. M., Kerman, I. A., Akil, H., Watson, S. J., & Sved, A. F. (2011). Novelty-seeking behavior predicts vulnerability in a rodent model of depression. *Physiology & Behavior*, *103*(2), 210–216. https://doi.org/10.1016/j.physbeh.2011.02.001

Sterner, E. Y., & Kalynchuk, L. E. (2010). Behavioral and neurobiological consequences of prolonged glucocorticoid exposure in rats: Relevance to depression. *Progress in Neuro-Psychopharmacology & Biological Psychiatry*, *34*(5), 777–790. https://doi.org/10.1016/j.pnpbp.2010.03.005

Stevens, B., & Johnson, M. B. (2021). The complement cascade repurposed in the brain. *Nature Reviews Immunology*, *21*(10), Article 10. https://doi.org/10.1038/s41577-021-00621-z

Subramanian, A., Tamayo, P., Mootha, V. K., Mukherjee, S., Ebert, B. L., Gillette, M. A., Paulovich, A., Pomeroy, S. L., Golub, T. R., Lander, E. S., & Mesirov, J. P. (2005). Gene set enrichment analysis: A knowledge-based approach for interpreting genome-wide expression profiles. *Proceedings of the National Academy of Sciences*, *102*(43), 15545–15550. https://doi.org/10.1073/pnas.0506580102

Sullivan, G. M., & Feinn, R. (2012). Using Effect Size—Or Why the P Value Is Not Enough. *Journal of Graduate Medical Education*, *4*(3), 279–282. https://doi.org/10.4300/JGME-D-12-00156.1

Szklarczyk, D., Franceschini, A., Wyder, S., Forslund, K., Heller, D., Huerta-Cepas, J., Simonovic, M., Roth, A., Santos, A., Tsafou, K. P., Kuhn, M., Bork, P., Jensen, L. J., & von Mering, C. (2015). STRING v10: Protein-protein interaction networks, integrated over the tree of life. *Nucleic Acids Research*, *43*(Database issue), D447-452. https://doi.org/10.1093/nar/gku1003

The UniProt Consortium. (2021). UniProt: The universal protein knowledgebase in 2021. *Nucleic Acids Research*, *49*(D1), D480–D489. https://doi.org/10.1093/nar/gkaa1100

Trachtenberg, A. J., Robert, J.-H., Abdalla, A. E., Fraser, A., He, S. Y., Lacy, J. N., Rivas-Morello, C., Truong, A., Hardiman, G., Ohno-Machado, L., Liu, F., Hovig, E., & Kuo, W. P. (2012). A primer on the current state of microarray technologies. *Methods in Molecular Biology (Clifton, N.J.)*, *802*, 3–17. https://doi.org/10.1007/978-1-61779-400-1_1

Treadway, M. T., Waskom, M. L., Dillon, D. G., Holmes, A. J., Park, M. T. M., Chakravarty, M. M., Dutra, S. J., Polli, F. E., Iosifescu, D. V., Fava, M., Gabrieli, J. D. E., & Pizzagalli, D. A. (2015). Illness Progression, Recent Stress and Morphometry of Hippocampal

Subfields and Medial Prefrontal Cortex in Major Depression. *Biological Psychiatry*, *77*(3), 285–294. https://doi.org/10.1016/j.biopsych.2014.06.018

Trunnell, E. R., & Carvalho, C. (2021). The forced swim test has poor accuracy for identifying novel antidepressants. *Drug Discovery Today*, *26*(12), 2898–2904. https://doi.org/10.1016/j.drudis.2021.08.003

Ueda, R., Yoshida, K., Kawakami, Y., Kawase, T., & Toda, M. (2004). Expression of a transcriptional factor, SOX6, in human gliomas. *Brain Tumor Pathology*, *21*(1), 35–38. https://doi.org/10.1007/BF02482175

Videbech, P., & Ravnkilde, B. (2004). Hippocampal Volume and Depression: A Meta-Analysis of MRI Studies. *American Journal of Psychiatry*, *161*(11), 1957–1966. https://doi.org/10.1176/appi.ajp.161.11.1957

Wang, Q., Timberlake, M. A., Prall, K., & Dwivedi, Y. (2017). The Recent Progress in Animal Models of Depression. *Progress in Neuro-Psychopharmacology & Biological Psychiatry*, *77*, 99–109. https://doi.org/10.1016/j.pnpbp.2017.04.008

Wang, X. (2016, March 7). *Next-generation sequencing data analysis*. https://doi.org/10.1201/b19532

Wei, Q., Fentress, H. M., Hoversten, M. T., Zhang, L., Hebda-Bauer, E. K., Watson, S. J., Seasholtz, A. F., & Akil, H. (2012a). Early-life forebrain glucocorticoid receptor overexpression increases anxiety behavior and cocaine sensitization. *Biological Psychiatry*, *71*(3), 224–231. https://doi.org/10.1016/j.biopsych.2011.07.009

Wei, Q., Fentress, H. M., Hoversten, M. T., Zhang, L., Hebda-Bauer, E. K., Watson, S. J., Seasholtz, A. F., & Akil, H. (2012b). Early-Life Forebrain Glucocorticoid Receptor

Overexpression Increases Anxiety Behavior and Cocaine Sensitization. *Biological Psychiatry*, *71*(3), 224–231. https://doi.org/10.1016/j.biopsych.2011.07.009

Wei, Q., Hebda-Bauer, E. K., Pletsch, A., Luo, J., Hoversten, M. T., Osetek, A. J., Evans, S. J., Watson, S. J., Seasholtz, A. F., & Akil, H. (2007). Overexpressing the Glucocorticoid Receptor in Forebrain Causes an Aging-Like Neuroendocrine Phenotype and Mild Cognitive Dysfunction. *Journal of Neuroscience*, *27*(33), 8836–8844. https://doi.org/10.1523/JNEUROSCI.0910-07.2007

Wei, Q., Lu, X.-Y., Liu, L., Schafer, G., Shieh, K.-R., Burke, S., Robinson, T. E., Watson, S. J., Seasholtz, A. F., & Akil, H. (2004). Glucocorticoid receptor overexpression in forebrain: A mouse model of increased emotional lability. *Proceedings of the National Academy of Sciences of the United States of America*, *101*(32), 11851–11856. https://doi.org/10.1073/pnas.0402208101

Wei, Y., Chen, T., Bosco, D. B., Xie, M., Zheng, J., Dheer, A., Ying, Y., Wu, Q., Lennon, V. A., & Wu, L.-J. (2021). The complement C3-C3aR pathway mediates microglia-astrocyte interaction following status epilepticus. *Glia*, *69*(5), 1155–1169. https://doi.org/10.1002/glia.23955

Widman, A. J., Cohen, J. L., McCoy, C. R., Unroe, K. A., Glover, M. E., Khan, A. U., Bredemann, T., McMahon, L. L., & Clinton, S. M. (2019). Rats bred for high anxiety exhibit distinct fear-related coping behavior, hippocampal physiology, and synaptic plasticity-related gene expression. *Hippocampus*, *29*(10), 939–956. https://doi.org/10.1002/hipo.23092

Wittstatt, J., Reiprich, S., & Küspert, M. (2019). Crazy Little Thing Called Sox—New Insights in Oligodendroglial Sox Protein Function. *International Journal of Molecular Sciences*, *20*(11), 2713. https://doi.org/10.3390/ijms20112713

Woo, J., Min, J. O., Kang, D.-S., Kim, Y. S., Jung, G. H., Park, H. J., Kim, S., An, H., Kwon, J., Kim, J., Shim, I., Kim, H.-G., Lee, C. J., & Yoon, B.-E. (2018). Control of motor coordination by astrocytic tonic GABA release through modulation of excitation/inhibition balance in cerebellum. *Proceedings of the National Academy of Sciences*, *115*(19), 5004–5009. https://doi.org/10.1073/pnas.1721187115

Yasumatsu, H. (1995). [Assessment of anxiolytics (4)—Social interaction test]. *Nihon Shinkei Seishin Yakurigaku Zasshi = Japanese Journal of Psychopharmacology*, *15*(4), 295–304.

Yoon, B.-E., Woo, J., Chun, Y.-E., Chun, H., Jo, S., Bae, J. Y., An, H., Min, J. O., Oh, S.-J., Han, K.-S., Kim, H. Y., Kim, T., Kim, Y. S., Bae, Y. C., & Lee, C. J. (2014). Glial GABA, synthesized by monoamine oxidase B, mediates tonic inhibition. *The Journal of Physiology*, *592*(Pt 22), 4951–4968. https://doi.org/10.1113/jphysiol.2014.278754

Yu, T., Guo, M., Garza, J., Rendon, S., Sun, X.-L., Zhang, W., & Lu, X.-Y. (2011). Cognitive and neural correlates of depression-like behaviour in socially defeated mice: An animal model of depression with cognitive dysfunction. *The International Journal of Neuropsychopharmacology / Official Scientific Journal of the Collegium Internationale Neuropsychopharmacologicum (CINP)*, *14*(3), 303–317. https://doi.org/10.1017/S1461145710000945

Zeisel, A., Hochgerner, H., Lönnerberg, P., Johnsson, A., Memic, F., van der Zwan, J., Häring, M., Braun, E., Borm, L. E., La Manno, G., Codeluppi, S., Furlan, A., Lee, K., Skene, N., Harris, K. D., Hjerling-Leffler, J., Arenas, E., Ernfors, P., Marklund, U., & Linnarsson, S.

(2018). Molecular Architecture of the Mouse Nervous System. *Cell*, *174*(4), 999-1014.e22. https://doi.org/10.1016/j.cell.2018.06.021

Zhou, B., Osinski, J. M., Mateo, J. L., Martynoga, B., Sim, F. J., Campbell, C. E., Guillemot, F., Piper, M., & Gronostajski, R. M. (2015). Loss of NFIX Transcription Factor Biases Postnatal Neural Stem/Progenitor Cells Toward Oligodendrogenesis. *Stem Cells and Development*, *24*(18), 2114–2126. https://doi.org/10.1089/scd.2015.0136

Zimmerman, M., Chelminski, I., & McDermut, W. (2002). Major depressive disorder and axis I diagnostic comorbidity. *The Journal of Clinical Psychiatry*, *63*(3), 187–193. https://doi.org/10.4088/jcp.v63n0303

Zimmerman, M., Martin, J., McGonigal, P., Harris, L., Kerr, S., Balling, C., Kiefer, R., Stanton, K., & Dalrymple, K. (2019). Validity of the DSM-5 anxious distress specifier for major depressive disorder. *Depression and Anxiety*, *36*(1), 31–38. https://doi.org/10.1002/da.22837

Ziylan, Z. Y., Bernard, G. C., Lefauconnier, J. M., Durand, G. A., & Bourre, J. M. (1992). Effect of dietary n-3 fatty acid deficiency on blood-to-brain transfer of sucrose, alpha-aminoisobutyric acid and phenylalanine in the rat. *Neuroscience Letters*, *137*(1), 9–13. https://doi.org/10.1016/0304-3940(92)90286-g

Appendix 1: Detailed Methods for The Individual Studies Included in the HDRF Database

The Glucocorticoid Receptor Overexpression (GRov) mouse model

Wei et al. 2007

Wei et al. 2007 examined the constitutive transgenic overexpression of the glucocorticoid receptor (GR) in the forebrain of mice (Wei et al., 2007). The reasoning behind the location-specific GR overexpression in the forebrain was to increase sensitivity in frontal brain regions to glucocorticoids such as corticosterone, which are released from the adrenal cortex in response to stress, without changing the sensitivity to GR in other parts of the brain and body important for the negative feedback that regulates glucocorticoid release. To produce this transgenic, they used PCR to introduce codons for the influenza hemagglutinin (HA) epitope to the 5' end of the full-length complementary DNA (cDNA) for GR. This HA-GR cDNA was under the control of the forebrain-specific promoter (CaMKIIa), so the HA-GR protein was specifically expressed in the forebrain. Properties of HA-GR, including fidelity and transactivation, were confirmed. The experimental groups tested in this study were hemizygote, GRov male mice (n=6), bred via breeding founders and progeny to C57BL/6J mice, as well as Wild Type (WT) male mice (n=6). All mice were exposed to light between 5:00 am to 7:00 pm on a 14/10 light/dark cycle and housed individually for one week preceding each study. To collect tissue for the microarray experiment, decapitation occurred in the morning at the age of 3-4 months, after one week of single housing. The tissue collection process included rapid dissection of the whole hippocampus, which was stored at -80°C prior to processing, and the collection of blood samples. Twenty seconds following decapitation, blood samples were promptly placed in iced Eppendorf tubes with EDTA. Microarray analysis was executed using the Affymetrix Mouse Genome 430_2.0 GeneChips (Affymetrix, Santa Clara, California) for transcriptional profiling, and the iScript cDNA synthesis kit (Bio-Rad, Hercules, CA) and Quant-It PicoGreen dsDNA kit (Invitrogen) for qRT-PCR. The preprocessing of the microarray data identified one outlier using Partek PCA analysis, leaving final sample sizes of GRov, n=5; WT, n=6 (Wei et al., 2007).

Wei et al. 2012

Wei et al. 2012 involved the inducible transgenic overexpression of the glucocorticoid receptor in the forebrain of mice (Wei et al., 2012). The reasoning behind the location-specific

GR overexpression in the forebrain was to increase sensitivity in frontal brain regions to glucocorticoids such as corticosterone, which are released from the adrenal cortex in response to stress, without changing the sensitivity to GR in other parts of the brain and body important for the negative feedback that regulates glucocorticoid release. The purpose of implementing the inducibility of this transgenic was to examine the effect of glucocorticoid sensitivity in frontal brain regions at specific developmental stages. Wei et al. generated this inducible GR overexpression in the forebrain by cloning HA-GR cDNA into the response plasmid tetracycline-response element (TRE) of the Tet-Off regulation system. The original HA-GR-TRE mice were then bred with CaMKII-tTA mice, causing tTA expression to target nervous tissue in the cortex, hippocampus, and striatum, due to the forebrain-specific promoter CaMKIIa controlling HA-GR cDNA expression. These bigenic, male mice were treated with Dox (200 mg/kg chow) to suppress overexpression of GR, and treatment was withdrawn during certain critical periods to allow for GR overexpression to occur. These groups consisted of lifetime expression of GRov (LT.GRov) (no Dox treatment), early life GRov (EL.GRov) (no Dox during postnatal weeks 1-3, but treated thereafter), and no GR overexpression (lifetime Dox treatment). The final group served as the experimental control due to lower levels of locomotor activity found from the CaMKII-tTA mice. For the microarray study, animals without experimental manipulation were used. These adult male mouse brains were collected in the morning with undisturbed conditions, then frozen, and later sliced. This tissue was cryostat-sectioned in the coronal plane at 12 μm. Using an AutoPix instrument, laser capture microdissection was used to obtain two brain regions: the hippocampal dentate gyrus (DG) and the nucleus accumbens (NAcc). The transcriptional profiling platform was the Affymetrix Mouse Genome 430_2.0 GeneChips. Microarray sample sizes were n=6 per group in the DG study and n=6-7 per group in the NAcc study (Lifetime GRov, n=7; early life GRov mice, n=6; no-GRov control mice, n=6) ((Wei et al., 2012), GEO# GSE30187).

The Flinders Sensitive Line (FSL) and Flinders Resistant Line (FRL) rat model

Blaveri et al. 2010

Blaveri et al. 2010 aimed to reveal the molecular mechanisms behind the behavioral differences in Flinders Sensitive Line (FSL) and Flinders Resistant Line (FRL) via profiling gene

expression in the hippocampus (HIP) and prefrontal/frontal cortex (P/FC) (Blaveri et al., 2010). Two independent cohorts were derived via a selective breeding strategy based on resistance and hypersensitivity to anticholinesterase diisopropylfluorophosphate (DFP), the latter being characteristic of depression. This breeding strategy utilized adult male Sprague-Dawley rats from the same colony yet bred six months apart, with cohort one including 12 FRL and 9 FSL animals, and cohort two including 10 FRL and 8 FSL animals, all of which lived under standard housing conditions. One week before microarray analysis, animals independently underwent the forced swim test. After this period of rest, the animals were decapitated, and the HIP and P/FC regions were swiftly excised on ice. The right hemisphere was set in RNA*later* (Qiagen, Inc., Valencia, CA, USA). RNA isolation, a process of homogenization, purification, quantification, and quality assessment, was completed using the following resources, respectively: TRIzol Reagent (Invitrogen Life Technologies, Carlsbad, CA, USA), RNeasy MiniKit (Qiagen, Inc., Valencia, CA, USA), Agilent 2100 bioanalyzer (Agilent Technologies, Palo Alto, CA, USA). The transcriptional profiling platform used in this study was the Affymetrix Rat Genome 230 2.0 GeneChips (Affymetrix, Santa Clara, CA). In an effort to circumvent any systematic error in tissue collection and sample processing, randomization schemes were used. The data from each cohort was organized into two batches of samples, separated by brain region, from which sample processing occurred in randomized order, equally distributed by line. All chips were then scanned and normalized using Rosetta Resolver Version 5.1 software (Rosetta Biosoftware, Seattle, WA, USA), and the data kept for continued analysis had a probeset normalized expression intensity greater than 30 in at least 50% of the samples per rat line ((Blaveri et al., 2010), GEO# GSE20388).

Bigio et al. 2016

Bigio et al. completed RNA sequencing of the ventral dentate gyrus (vDG) of the FSL vs. FRL depression model, with an adjacent look at the impact of responsiveness to the epigenetic molecule acetyl-L-carnitine (LAC) (Bigio et al., 2016). The animals studied were adult male FSL and FRL rats in standard housing in groups of four of the same genotype. Temperature and humidity were held at a constant 22 ±1° C, and rats were kept on a 12-hr light/dark cycle. The goal of this study was to identify genes that fall into three categories: predisposition to depression, response to acetyl-L-carnitine (LAC), or resistance to a low dose of LAC in Flinders

Sensitive Line rats (FSL) following acute stress from treatment. The LAC molecule has been shown to have antidepressant effects in FSL rats by establishing a normal energy homeostasis via regulation of mitochondrial metabolism and realignment of glutamate imbalance in the hippocampus. The adult male FSL and FRL rats were administered either a dosage of LAC (sigma, concentration of 0.3% wt/vol) or tap water (vehicle) via the rat sipping bottles, which was available for seven days. During the last two days of treatment, the animals underwent behavioral testing, including an Open Field test on the sixth day, as well as a five-minute forced swim test (FST) on the seventh. Based on immobility times to the FST, FSL rats treated with LAC were divided into two groups: response (rFSL) and no response (nrFSL). The former group was categorized by an immobility time within 1 standard deviation of the mean of the control veh-FRL group. FSL rats with times that did not make this cutoff were placed in the nrFSL group. Directly after the FST, the animals were sacrificed by decapitation with brief exposure to a CO2 saturated chamber just prior. The vDG tissue was dissected and weighed, first by slicing using the brain matrix, and then by punch with 130 mg lysed, and the tissue was then homogenized. Extraction of the RNA was completed using the Qiazol reagent and RNeasy mini (Qiagen). The Agilent 2100 Bioanalyzer was used to assess RNA integrity, and the Illumina HiSeq2500 was used for sequencing. RNA-seq sample sizes were n=3 per the following groups: rFSL, nrFSL, vehicle FSL, and vehicle FRL ((Bigio et al., 2016), GEO# GSE83336).

The CORT/Fluoxetine mouse model

Samuels et al. 2014

Samuels et al. investigated gene expression in the dentate gyrus (DG) on a mouse model of depression induced by chronic corticosterone (CORT) treatment (Samuels et al., 2014). This model involved male C57BL/6Ntac mice treated with corticosterone (35 ug/ml) dissolved in vehicle (0.45% beta-cyclodextrin) at 7–8 weeks old, treated for 21 days. This served as the control group (n=15). The treatment group (n=15) received CORT combined with fluoxetine (FLX, 160 ug/ml), a selective serotonin reuptake inhibitor (SSRI) commonly used as a medication for major depression. The animals were kept on a 12:12 light/dark cycle in groups of five per cage, and drug delivery occurred through drinking water in opaque bottles. Serum levels of a separate cohort of animals treated for 21 days with fluoxetine were tested to check for a

comparable amount of norfluoxetine (a metabolite of fluoxetine) across all mice. The animals tested in the microarray study also underwent behavioral testing following the drug treatment, in the form of the Novelty Suppressed Feeding Test (NSF) and Forced Swim Test (FST) four days apart, respectively. The NSF test measures determined grouping of animals into "responders" or "resistant" categories. Only the eleven out of the fifteen mice treated with FLX that showed both decreased anxiety on the NSF and decreased behavioral despair on the FST were evaluated using microarray, and eight out of the fifteen control mice were randomly selected for comparison. A week following behavioral testing, while being maintained on drug treatments, the mice were sacrificed. The brains were collected whole and kept in chilled artificial cerebrospinal fluid (ACSF) for five minutes, and then the hippocampus was removed and sliced transversely along the septotemporal axis. From these slices, both the molecular and granular layers of the dentate gyrus were microdissected. Bilateral dentate gyri were combined into RNase free microcentrifuge tubes for each of the dorsal and ventral dissections. All tissue samples were stored at -80 degrees Celsius and RNA was isolated using lysis buffer (Qiagen Rneasy kit) and a homogenizer. Microarrays represent data from the dentate gyrus. All samples were processed in parallel and hybridized in a single batch using Affymetrix 430_2 39 expression arrays. The final sample sizes for microarray were n=11 for the FLX treatment groups and n= 8 for the non FLX-treated control groups for both the ventral and dorsal dentate gyrus ((Samuels et al., 2014), GEO# GSE43261).

The Chronic Social Defeat Stress (CSDS) mouse model

Bagot et al. 2016

Bagot et al. aimed to understand the molecular mechanisms underlying the dysregulated circuitry in depression (Bagot et al., 2016). This study used the chronic social defeat stress (CSDS) mouse model to generate transcriptional profiles using RNA sequencing of control (no stress), susceptible, and resilient mice at three points in time following the CSDS paradigm. The mice in this experiment were male, 6-8 week-old C57BL/6J mice housed five per cage (excluding during social defeat in which they were housed alone) on a 12:12h light-dark cycle, with lights on at 7 am. The chronic stress paradigm was created by subjecting the treatment group to daily, five-minute intervals of social defeat for ten days. The mice at eight weeks of age

were paired with an aggressor mouse at six months old. This was followed by housing the victim beside the aggressor, separated only by plexiglass, for the continuation of that day. The purpose of this housing situation was to continue one form of sensory stimulation leading to stress. Control mice were rotated daily among housing across plexiglass barriers with another control mouse as well. The mice were then divided into the stress susceptible or resilient groups based on their inclination to social interaction with a novel mouse following the ten social defeat experiences. In a two-stage social interaction test, the resilient group was defined as animals that maintained an interest in social interaction with a novel mouse, while the susceptible group avoided social interaction. Following the CSDS paradigm, the animals were sacrificed at varying times including both early, late, and late + stress-primed times to provide insight into the dynamics of these two phenotypes, susceptible or resilient, over time. The early group was sacrificed directly from their cage 48 hours post-defeat, the late group sacrificed 28 days subsequently, and the final group sacrificed 28 days and 1-hour post-defeat, following an additional five-minute re-exposure to an aggressor mouse. After each sacrifice, the brains were laid in a mold with approximately 1 millimeter thick sections created with razor blades. Then, 15 g punch dissections were taken from four brain regions (the nucleus accumbens (NAC), ventral hippocampus (VHIP), prefrontal cortex (PFC), and amygdala (AMY)) and flash frozen. The RNA-seq sample sizes were n=3 (early, 48hr) n=4 (late, 28 day) and n = 4 (28d + 1hr) for all four regions. RNA was sequenced with 100 base pair single-end reads ((Bagot et al., 2016), GEO# GSE72343).

Bagot et al. 2017

Bagot et al. investigated the effects of ketamine, a dissociative anesthetic, as an antidepressant in a side-by-side comparison to the effects of the longstanding tricyclic antidepressant imipramine (Bagot et al., 2017). Ketamine was chosen for its unknown mechanism at lower dosages, in contrast to its widely understood anesthetic and recreational uses. Bagot et. al used the chronic social defeat stress (CSDS) model with C57BL/6J male 8-week old mice by exposure to 10 daily, 5-min defeat sessions by a novel aggressor mouse. Mice were kept on a 12:12h light-dark cycle, with lights on at 7 a.m., and housed 5 per cage until the social defeat experience at which point onward they were single-housed. This housing included a plexiglass divider between the experimental mouse and its aggressor for continued visual stress

stimulation. Twenty-four hours following the final social defeat, mice were subjected to a two-stage social interaction test, the results of which determined the grouping of the mice into either stress-susceptible or stress-resilient mice, the latter defined as spending more time in an "interaction zone" of an enclosure when it contained a novel CD1 mouse than when it was empty. Subsequently, the susceptible mice were divided into thirds and administered one of three treatments: either imipramine (20 mg/kg), ketamine (10 mg/kg), or saline. Imipramine and saline treatments were administered via i.p. injection once daily for fourteen days. Ketamine, however, was administered acutely due to prior evidence of effective treatment. Thus, the susceptible mice in the ketamine treatment group received saline i.p. injections for the first 13 days and one ketamine injection on the fourteenth day. Resilient and control mice also received saline treatments. Another social interaction test followed twenty-four hours after the final treatment to distinguish "responders" and "nonresponders" to their respective treatments. Responders were defined as subjects that spent more time interacting with the novel mouse after treatment and showed an increase of > 20 seconds in interaction time compared to the first SI test. Non-responders were defined as having spent less time interacting with the target or increased less than 10 seconds of interaction time. The subjects were killed two days thereafter in order to profile resting-state expression without the interference of effects from the behavioral testing. The mouse brains were removed, coronally sliced, dissected, and frozen on dry ice. Micro-dissections were performed by placing brains in a brain mold with ~1mm thick sections created with razor blades. Then 15 g punch dissections are taken from each region, then rapidly frozen until use The regions dissected include the nucleus accumbens (NAC), ventral hippocampus (VHIP), prefrontal cortex (PFC), and amygdala (AMY). RNA was sequenced on the Illumina HiSeq 2500 System with 50 base pair paired-end reads. Sample sizes were between n=3-5 for each group (see **Table 1** for exact sample sizes) ((Bagot et al., 2017), GEO# GSE81672).

Caradonna et al. 2022

This publication includes a study investigating the effects of enriched vs. standard housing on the chronic social defeat stress model. The C57BL/6J experimental mice experienced either enrichedor standard housing on a 12-h light-dark cycle (lights off 7:00pm). Enriched housing consisted of 12 mice per 78x86cm cage with tunnels, running wheels, and novel inanimate objects, all of which were cleaned weekly and rearranged according to eight unique

layouts. For standard housing, mice were housed three per 30x18cm standard cage. Aggressor CD-1 mice were selected based on attacking a novel C57BL/6J mouse at least twice within the first 60 seconds of this screening procedure. Following the third screening, the aggressor mice were left in the standard rat cage with a plexiglass divider and social defeat of the intruding mice occurred the next day. After 8 weeks of enriched or standard housing exposure, the CSDS paradigm was conducted for 10 consecutive days, 5–10 min/per day, after which the intruder was placed behind the perforated plexiglass divider for the remainder of the 24-hour period. Each social defeat occurred with a novel aggressor mouse. Control animals were housed in identical cage setups with two animals per cage, separated by the clear, perforated divider for the same duration as the social defeat experiences. Twenty four hours following the final defeat, social interaction testing was conducted. Subjects were given 150 seconds to explore the arena before the novel CD-1 aggressor was placed in the wire-mesh box inside the arena. Mice were divided into stress-resilient and stress-susceptible groups based on the ratio of time spent inside vs. outside of the interaction zone of the arena. At P80, mice were sacrificed by cervical dislocation and rapid decapitation. The brains were extracted whole, flash frozen, and later coronally and horizontally sliced. The ventral dentate gyrus region was punch-dissected using a 300 μm diameter puncher. RNA sequencing was conducted using the Illumina HiSeq 2500. cDNA libraries consisted of 100bp paired-end reads. Sample sizes by treatment group were the following: Enriched-Control n=10, Standard-Control n=10, Enriched-Resilient n=9, Standard-Resilient n=7, Enriched-Susceptible n=9 Standard-Susceptible n=10 ((Caradonna et al., 2022), GEO# GSE150812).

The Bred Low Responder (bLR) and Bred High Responder (bHR) rat model

Birt, Hagenauer, et al. 2021

Birt et al. studied differences in hippocampal gene expression in the bred-High Responder (bHR) and bred-Low Responder (bLR) rat model (Birt et al., 2021). They used a selective breeding strategy based on exploratory locomotor activity in a novel environment to produce temperamental extremes. The first generation of animals were Sprague-Dawley rats that were bred using the top and bottom 20% of locomotor testing scores in order to emphasize the differences in phenotype. The bHR group demonstrates a phenotype representative of aggressive,

exploratory, and reward-seeking behavior, while bLR exhibits anxious, markedly less exploratory, depressive-like behavior. Using this paradigm, selective breeding continued for almost two decades. At the beginning of the postnatal period, the animals were housed with twelve pups (equal gender ratio) and one dam. In early development, the rats lived in a 14:10 light:dark cycle, with lights on at 4 a.m., until postnatal day 21 (after weaning) at which point the animals were kept on a 12:12 light:dark schedule, with lights on 6 a.m. Additionally, after weaning, the animals were housed in groups of 2-3 other pups. Around P50-P75, locomotor test scores were obtained from the animals. This testing occurred in the morning using standard, clear acrylic cages (similar to the original housing) in a separate room (Birt et al., 2021).

Two RNA-seq experiments were conducted with slightly differing protocols. The first (MBNI_RNASeq_F37) was conducted on male bLR and bHR adults in the 37th generation of selective breeding. Uniquely, this study incorporated the breeding of HR and LR groups to include rats exhibiting intermediate locomotor responses (bIR) to the novel environment. The sample sizes were n=6 per group. Additional behavioral testing, along with the locomotor test, included anxiety testing using the Elevated Plus Maze (EPM). This consisted of placing the animals in a plexiglass device 70 cm above the floor. The shape of the maze resembled a plus sign, with two branches, or arms, having 45 cm walls erected on either side, while the other two arms did not. In order to quantitatively measure anxiety-like behavior, the percentage of time in any of the areas of this maze was monitored and recorded in one of three categories: open arms, closed arms, and the intersection between the two (also without walls). These animals were then sacrificed by decapitation at the ages of P160-P167 for the bHR and bLR groups, and P126-134 for the bIR group. The hippocampus was removed whole and rapidly frozen. The MBNI_RNASeq_F37 was sequenced on the Illumina HiSeq 2000 with paired-end 100 base pair sequencing. Sample sizes were n=6 per group ((Birt et al., 2021), GEO# GSE140598).

The second RNA-seq study, involving the 43rd generation of the selective breeding strategy of bHR and bLR animals (MBNI_RNASeq_F43) tested social interaction soon after the animals experienced 15 minutes of anxiety-inducing time on the open arms of the EPM. The animals were kept in standard housing conditions. The social interaction test went as follows: experimental rats were placed in a rectangular box with an open top, inside of which was a similar, novel stimulus rat (similar age, size, species, with no prior contact). In dim lighting, the rats were monitored for time spent interacting, described as the experimental rat initiating social

contact through sniffing, following, or touching. This testing spanned five minutes. An hour following the time of the earlier EPM, the rats were sacrificed by decapitation and the brains were flash frozen. Later on, the hippocampus was dissected whole. RNA extraction was carried out using the Zymo RNA isolation Kit. The MBNI_RNASeq_F43 was sequenced on the Illumina HiSeq 2000 at 50-bp length for non-stranded short-read. Sample sizes were n=5 per group ((Birt et al., 2021), GEO# GSE140287).

The BDNF Val66Met Mouse Model

Marrocco et al. 2020

Marrocco et al. investigated the genetic factors involved in Premenstrual Dysphoric Disorder (PMDD), a condition including symptoms of anxiety and depression (Marrocco et al., 2019). To do so, they used mice with a single nucleotide polymorphism (SNP) of the human brain-derived neurotrophic factor gene (BDNF) and treated them with estradiol, a hormone that has been proven to affect the behavior and mice from this model. The BDNF gene has shown association with anxiety and estrogen-dependent hippocampal function. The SNP at this gene causes a change of amino acids at position 66 from Val to Met. These mice were generated at a separate laboratory and, using in-house breeding, generated Wild-type C57/BL6 mice (WT) and heterozygous BDNF Val66Met knock-in mice (Het-Met). The animals were housed in groups of 4–5 in standard cages on a 12-h light-dark cycle, with lights off 7:00 pm. Around P75-80, the mice were ovariectomized in a process that included anesthetic treatment using a solution of ketamine (75 mg kg-1) and xylazine (7.5 mg kg-1). Small incisions were made on each flank to remove the ovaries. Two weeks following the ovariectomy, the mice were behaviorally tested for the effects of estradiol (E2). The female mice were randomly assigned to either control or estradiol treatment groups. In both cases, the researchers administered treatment *ad libitum* through the subjects' drinking water. The dosages were as follows: 300 nM β-E2 in 0.1% ethanol (0.7 g/day) for the experimental group, or 0.1% ethanol (vehicle) solution for the control group. Treatment continued for six weeks. At week three, the mice began testing for anxiety-like and depression-like behaviors through the Open Field Test and Splash Test. In the Open Field Test, the mice were observed in an empty, square arena for ten minutes. The mice were recorded and observed for the time spent in the center of the arena, the total distance moved, the number of

visits to the center of the arena, and the time spent in the corner. In the Splash Test, after a 30 minute habituation period to the new cage, the mice were removed from the cage, sprayed from behind using a 10% (w/v in water) sucrose solution, and analyzed for grooming behaviors. Following treatment, the mice were killed by cervical dislocation and rapid decapitation. The hippocampi were extracted, the uteri were removed, and the vHpc was isolated. The Qiagen Lipid Tissue Mini Kit (ThermoFisher, Waltham, MA, USA) was used for RNA extraction from ventral hippocampal tissue. For the RNA sequencing study, each group was represented by three biological replicates, including RNA pooled from two animals each. 200 ng per group of RNA was prepared. Using an Illumina NextSeq 500, the cDNA libraries were sequenced in a single lane. 75-bp single-end reads were generated per sample ((Marrocco et al., 2020), GEO# GSE121412).

Caradonna et al. 2022

This study included an experiment within it that examined the effects of corticosterone (CORT) on the ventral hippocampus of the BDNF Val66Met mouse model using RNA-sequencing. The animals in this study were provided standard housing in groups of n=4-5/group on a 12:12-h light-dark cycle (lights off 7:00pm). Chronic CORT treatment (25 μg/ml corticosterone dissolved in ethanol, and diluted in tap water to 1% concentration) was administered through drinking water for six weeks, and began when the animals were two months old. WT and BDNF Val66Met mice were randomly assigned to either vehicle or CORT treatment groups.

After three weeks of CORT treatment, the mice underwent behavioral testing, including the Light-Dark Box Test and Splash Test. The Light-Dark Box Test consisted of five minutes in which the animals' inclination towards light and dark boxes inside the arena was recorded, including time spent inside the light box, latency to go into the dark box, and latency to return to the light box. In the Splash Test, the animals were sprayed with a 10% sucrose solution on the hindquarters and had grooming behaviors monitored for five minutes. The mice were killed following the six week CORT treatment by cervical dislocation and rapid brain extraction, as well as an immediate dissection of the ventral hippocampus. Sequencing was completed using an Illumina NextSeq 500 to obtain 75-bp single-end reads. Sample sizes were n=3 per group ((Caradonna et al., 2022), GEO# GSE174664).

Appendix 2: Unpublished Methods for the Custom Gene Set File (written by Dr. Megan Hagenauer)

The custom gene set file was designed to provide greater insight into differential expression results related to mood disorder than simple functional ontology, and had been constructed as part of a previous unpublished project. For this project, we trimmed out some of the gene sets specific to other brain areas, leaving the following. We included gene sets from three commonly-used collections on the Molecular Signatures Database (Subramanian et al., 2005) (MSigDB v7.3, http://software.broadinstitute.org/gsea/msigdb/index.jsp, downloaded 2021-03-25): the full traditional Gene Ontology annotation database ("C5: GO Gene Sets", file: "c5.all.v7.3.symbols.gmt.txt", # of gene sets: 14,996), as well as two other databases that were subsequently filtered for relevance to central nervous system tissue: the curated gene set database ("C2: Curated Gene Sets", file: "c2.all.v7.3.symbols.gmt.txt", # of filtered gene sets: 158) and the cell type database ("C8: Cell Type Signature Gene Sets", file: "c8.all.v7.3.symbols.gmt.txt", # of filtered gene sets: 211).

To these gene sets, we added our own custom gene sets that were designed to specifically provide insight into hippocampal function within our experimental design. We first added a set of custom gene sets that had been previously curated (Birt et al., 2021) (# of gene sets: 69) to target hippocampal regional gene expression signatures (Cembrowski et al., 2016) and hippocampal co-expression networks (Johnson et al., 2015; Park et al., 2011).

Next, we extracted gene sets enriched for expression within specific brain cell types from the BrainInABlender database (Hagenauer et al., 2018) (*https://github.com/hagenaue/BrainInABlender*, v.0.0.0.9000, # of gene sets: 39) and the DropViz database of scRNA-Seq results from hippocampal tissue (Saunders et al., 2018) (http://dropviz.org, parameters: Cell Type Cluster vs. Rest of Region: p-value< 10^{-30}, minimum fold ratio=4, minimum logCPM in Cell Type Cluster=0.5, maximum logCPM in Rest of Region=6). To increase conciseness and specificity, the gene sets associated with the hippocampal cell type clusters from the DropViz database were further filtered to include either 1) all genes with fold change greater than 10 for the cluster vs. the rest of the region (if there were more than 50 genes meeting these criteria), or 2) The top 50 genes with the highest fold change for the cluster vs. the rest of the region (# of gene sets: 13).

We next curated gene sets derived from chronic restraint stress, forced swim stress, and acute corticosterone in the HC (Gray et al., 2014) ($p<0.005$ for any of the individual comparisons, divided into upregulated and down-regulated for each comparison, or $p<0.00005$ for an ANOVA encompassing all conditions) (# of gene sets: 9).

We next added gene sets from hippocampal transcriptional profiling studies examining the effects of selective breeding targeting internalizing behavior (Andrus et al., 2012; Birt et al., 2021; Blaveri et al., 2010; Díaz-Morán et al., 2013; Garafola & Henn, 2014; Raghavan et al., 2017; Sabariego et al., 2013; Wilhelm et al., 2010; Zhang et al., 2005). These differentially expressed gene lists had been curated in a previous publication (Birt et al., 2021) using their original publication-specific criteria to define significance. We created up-regulated and down-regulated versions of each gene set when there were sufficient differentially expressed genes (>10, # of gene sets: 14).

Finally, we compiled a set of gene sets related to human neuropsychiatric disorders (Major Depressive Disorder, Bipolar Disorder, Schizophrenia, Autism Spectrum Disorder, Alcohol Abuse Disorder) using the differentially expressed genes identified in a recent large meta-analysis of cortical transcriptional profiling studies (Gandal et al., 2018) (FDR<0.05 & $p<0.001$). Each of these gene sets was divided into down-regulated and upregulated genes (# of gene sets: 14).

We extracted gene sets from two online databases of differential expression results: Gemma (https://gemma.msl.ubc.ca/home.html, (*Gemma: A Resource for the Reuse, Sharing and Meta-Analysis of Expression Profiling Data | Bioinformatics | Oxford Academic*, n.d.)) and GeneWeaver (https://www.geneweaver.org,(Baker et al., 2012)), For GeneWeaver, public experimentally-derived gene sets from the nucleus accumbens or hippocampus from studies related to stress, environmental enrichment, affective behavior, and mood disorder were extracted from the website. The results were ranked by the differential expression metric provided (FDR, p-value or absolute effect size), and the gene symbol annotation for either the full or top 25 results was extracted, ignoring results lacking gene symbol annotation or mapped to multiple gene symbols (n=38 gene sets, NACC=5, HC=33).

For Gemma, we used gemmaAPI (Github: *PavlidisLab/gemmaAPI.R*) to access results. We used *annotationInfo()* to download a list of all datasets including the annotation “nucleus accumbens” or “hippocampus”, and narrowed that list to public datasets from humans, mice, or

rats that weren't tagged as troubled (NACC: 103 datasets, HC: 648 datasets). Datasets that were tagged as having batch confounds were reviewed by hand to ascertain whether the confound would interfere with the interpretation of the variable of interest (e.g., effect of stress, treatment). Datasets were then further reviewed by hand for relevance to stress, environmental enrichment, affective behavior, and mood disorder (NACC: 15 datasets, HC: 86 datasets).

The results for the datasets of interest were then downloaded locally. The "analysis.results.txt" file for each dataset, which included the p-values and q-values for each variable in the dataset for each transcript/gene, was extracted and joined with the "resultset" for each variable, which included the FoldChange, T-stat, and P-value outputted for each contrast, using the database unique gene identifier ("Element_Name"). These results were then filtered to remove results that either lacked gene symbol annotation or that had mapped to multiple gene symbols (separated by a "|" in the database). These files were then subsetted to pull out results for each variable that survived a threshold of FDR<0.10 and p-value<0.0001, and then the results for the specific contrasts for that variable were further filtered using p<0.05. The down-regulated (FoldChange<1) and up-regulated (FoldChange>1) results were divided into separate gene sets. These gene sets were then ranked by FoldChange, and only the 999 most down-regulated and up-regulated transcripts were maintained in the gene set. The final database included 329 gene sets (NACC: 28, HC: 301).

For all custom gene sets, gene symbol annotation was obtained from the original study/database or using relevant annotation packages (*org.Hs.egSymbol v.3.4.1, org.Mm.egSymbol v.3.4.1, org.Rn.egSymbol v.3.4.1*). Only unique gene symbols were included in the final gene set (no duplicates). Genes with older, problematic date-related symbols (March genes, Sept genes, Dec genes, Nov) were identified and changed to updated nomenclature. Then, when appropriate, rat orthologs for the genes included in each gene set were identified using the ortholog database on the Mouse Genome Initiative (MGI) website (Bult et al., 2019) (http://www.informatics.jax.org/homology.shtml, downloaded 02/28/2021).